

ANALYSIS OF A BACKWARD EULER-TYPE SCHEME FOR MAXWELL'S EQUATIONS IN A HAVRILIAK-NEGAMI DISPERSIVE MEDIUM

YUBO YANG¹, LI-LIAN WANG² AND FANHAI ZENG³

ABSTRACT. For the Maxwell's equations in a Havriliak-Negami (H-N) dispersive medium, the associated energy dissipation law has not been settled at both continuous level and discrete level. In this paper, we rigorously show that the energy of the H-N model can be bounded by the initial energy so that the model is well-posed. We analyse a backward Euler-type semi-discrete scheme, and prove that the modified discrete energy decays monotonically in time. Such a strong stability ensures that the scheme is unconditionally stable. We also introduce a fast temporal convolution algorithm to alleviate the burden of the history dependence in the polarisation relation involving the singular kernel with the Mittag-Leffler function with three parameters. We provide ample numerical results to demonstrate the efficiency and accuracy of a full-discrete scheme via a spectra-Galerkin method in two spatial dimension. Finally, we consider an interesting application in the recovery of complex relative permittivity and some related physical quantities.

1. INTRODUCTION

In electromagnetism, the most general model for a dispersive dielectric material, i.e. a material with frequency-dependent permittivity, is the Havriliak-Negami (H-N) dielectric model (see, e.g., [18, 19, 21, 34]). In this model, the complex relative permittivity is expressed as

$$\epsilon_r(\omega) = \epsilon_\infty + \frac{\epsilon_s - \epsilon_\infty}{(1 + (i\omega\tau_0)^\alpha)^\beta}, \quad (1.1)$$

where $0 < \alpha, \beta \leq 1$, $\epsilon_\infty, \epsilon_s$ and τ_0 are the infinite-frequency permittivity, the static permittivity and the relaxation time respectively, and $\epsilon_s, \epsilon_\infty$ satisfy $\epsilon_s > \epsilon_\infty \geq 1$. Furthermore, $i = \sqrt{-1}$ denotes the imaginary unit, and ω is the angular frequency. All the anomalously dispersive dielectric models are its subclasses. When $\alpha = \beta = 1$, the H-N model reduces to the Debye model [9], while the H-N model reduces to Davidson-Cole (D-C) model [8] when $\alpha = 1$, and to Cole-Cole (C-C) model when $\beta = 1$ [7]. Such models arise from diverse fields, which typically include biological tissues [31, 4, 25], soils [38], amorphous polymers near the glass-liquid transition [12], glassy materials [1] among others.

In general, there are two main strategies to simulate the electromagnetic wave propagations in dispersive media based on different treatments of the relation between the electric flux and electric field intensity, governed by the polarisation equation. The first is to introduce certain auxiliary function and related auxiliary differential equation (ADE) to deal with the polarisation. The second is to formulate the polarisation as a time convolution integral equation of the electric field. For the Debye or Debye-type model, such as Drude or Lorentz model, its time-domain expression of its relative complex permittivity can be easily formulated, because its relative complex permittivity is a function of integer powers of $i\omega$. Therefore, both approaches can be applied. In particular, the ADE involves derivatives of integer

2010 *Mathematics Subject Classification.* 65N35, 65E05, 65N12, 41A10, 41A25, 41A30, 41A58.

Key words and phrases. Maxwell's equations, Havriliak-Negami dispersive medium, strong stability, unconditionally stable scheme, fast temporal convolution algorithm.

¹Nanhu College, Jiaxing University, Jiaxing, Zhejiang 314001, China. Email: boydman_xm@zjxu.edu.cn.

²Division of Mathematical Sciences, School of Physical and Mathematical Sciences, Nanyang Technological University, 637371, Singapore. Email: lilian@ntu.edu.sg. The research of this author is partially supported by Singapore MOE AcRF Tier 1 Grant (RG 15/12), and Singapore MOE AcRF Tier 2 Grants (MOE2017-T2-144 and MOE2018-T2-1-059).

³School of Mathematics, Shandong University, Jinan, Shandong 250100, China. Email: fanhai_zeng@sdu.edu.cn.

The first author would like to thank NTU for hosting his visit devoted to this collaborative work.

order that can be discretised by the finite difference methods [42, 11] as usual. However, the relative complex permittivity of the H-N, D-C or C-C model involves a function of non-integer powers of $i\omega$, so its representation in the time domain is much more complicated. In fact, the polarisation relations are oftentimes integro-differential equations with global fractional operators [30, 24, 37, 20, 5], which pose significant difficulties and are much more expensive to solve.

In regards to the C-C model, fractional ADE-based time-domain methods were proposed in e.g. [24, 35, 40, 43], where the polarisation equation involves the fractional-in-time Riemann-Liouville derivative (cf. [30]). As such, much recent development in numerical fractional differential equations casts light on time discretisation of this model. However, there has been very limited works on numerical solutions of the D-C and H-N models, largely due to that the polarisation relation cannot be expressed in terms of ADE with usual fractional differential operators. Nevertheless, some interesting attempts include the approximation of the D-C or H-N model by the Debye model in the frequency domain [37, 36, 22, 6]; or by the C-C model in the frequency domain [39, 28, 3, 2]. We remark that most works related to H-N, C-C or D-C model above are implemented by the finite difference time-domain (FDTD) method (cf. [42]), and the stability and convergence analysis is yet unavailable. On the other hand, Li et al. [24], and Huang and Wang [20] developed a finite element time-domain (FETD) method (based on a fractional differential form of the polarisation equation) and a spectral time-domain method (based on an integro-differential formulation) for the C-C model, respectively. Stability and convergence analysis were also provided in their works.

In this paper, we propose and analyse a time-domain numerical method for solving the H-N model with the polarisation relation formulated by an integral equation involving a singular kernel function in terms of the Mittag-Leffler (ML) function with three parameters. We highlight our main contributions as follows.

- With the aid of some useful properties of the ML function, we prove that the energy of the H-N model can be controlled by the initial energy, which ensures the well-posedness of the model and plays an important role in developing stable numerical methods.
- We conduct a delicate and rigorous analyse of a semi-discrete scheme which can incorporate various spatial discretisation. More precisely, we propose a first-order backward-Euler-type scheme, and show for the first time that the discrete energy (with a modification of the continuous energy by adding a history part) decays monotonically. This strong stability guarantees that the scheme is unconditionally stable and is essential for the convergence analysis. However, it appears non-trivial to show this if one works with the fractional differential form of the polarisation relation in the context of the C-C model [24].
- A fast temporal convolution algorithm for the H-N model is realised by following some basic ideas in [26, 45], which requires $O(\log N_t)$ storage and $O(N_t \log N_t)$ operations over N_t time steps, when only cost in time direction is considered. Here, N_t represents the total number of time steps. Note that the direct implementation of the scheme (3.2) would require $O(N_t)$ storage and $O(N_t^2)$ operations, which is computational expensive and forms a bottleneck for long time simulation.

The rest of this paper is organised as follows. In the next section, we introduce the Havriliak-Negami dispersive dielectric model, and conduct the stability analysis. In section 3, we propose a time discrete scheme for the H-N model, and provide its stability and error analysis. In section 4, we implement a fast temporal convolution algorithm, and illustrate spatial discretisation through a two-dimensional H-N model. Then we supply with ample numerical results to demonstrate the efficiency and accuracy of the proposed scheme. Finally, we conclude the paper with an interesting application in the recovery of the complex relative permittivity and some related physical quantities.

At the end of this section, we introduce some notations to be used throughout the paper. Let C (sometimes with a subindex) denote a generic constant independent of the time step size Δt and the space parameter N . For $r \geq 0$, let $H^r(\Omega)$ (resp. $\mathbf{H}^r(\Omega)$) be the usual Sobolev space with $H^0(\Omega) = L^2(\Omega)$ (resp. $\mathbf{H}^0(\Omega) = \mathbf{L}^2(\Omega)$) for the scalar (resp. vector-valued) functions on a bounded domain Ω with

Lipschitz boundary. As usual, we denote the inner product and norm of both $L^2(\Omega)$ and $\mathbf{L}^2(\Omega)$ by (\cdot, \cdot) and $\|\cdot\|$, respectively. Given a Hilbert space \mathbf{X} with the norm $\|\cdot\|_{\mathbf{X}}$, we define the space $L^\infty(0, T; \mathbf{X})$, $L^2(0, T; \mathbf{X})$ with the norm

$$\|\mathbf{U}\|_{L^\infty(0, T; \mathbf{X})} = \operatorname{ess\,sup}_{0 \leq t \leq T} \|\mathbf{U}(\cdot, t)\|_{\mathbf{X}}, \quad \|\mathbf{U}\|_{L^2(0, T; \mathbf{X})} = \left(\int_0^T \|\mathbf{U}(\cdot, t)\|_{\mathbf{X}}^2 dt \right)^{1/2}.$$

Furthermore, we define

$$H^k(0, T; \mathbf{X}) \triangleq \{\mathbf{v} \in L^2(0, T; \mathbf{X}) : \partial_t^\ell \mathbf{v} \in L^2(0, T; \mathbf{X}), \ 1 \leq \ell \leq k\}$$

with the norm $\|\cdot\|_{H^k(0, T; \mathbf{X})}$, and $C^m(0, T; \mathbf{X})$ be the space of m times continuously differentiable functions from $[0, T]$ into the Hilbert space \mathbf{X} (cf. [33]). We also use some common notations (cf. [29])

$$H(\operatorname{curl}; \Omega) = \{\mathbf{v} \in \mathbf{L}^2(\Omega); \nabla \times \mathbf{v} \in \mathbf{L}^2(\Omega)\}, \quad H_0(\operatorname{curl}; \Omega) = \{\mathbf{v} \in H(\operatorname{curl}; \Omega); \mathbf{n} \times \mathbf{v} = \mathbf{0} \text{ on } \partial\Omega\}.$$

2. THE HAVRILIAK-NEGAMI DISPERSIVE DIELECTRIC MODEL

In an H-N medium, the time-domain Maxwell's equations take the form (cf. [18, 19]):

$$\epsilon_0 \epsilon_\infty \partial_t \mathbf{E} = \nabla \times \mathbf{H} - \partial_t \mathbf{P}, \quad \mu_0 \partial_t \mathbf{H} = -\nabla \times \mathbf{E} \quad \text{in } \Omega \times (0, T], \quad (2.1)$$

where $\mathbf{P}(\mathbf{x}, t)$ is the induced electric polarisation given by

$$\mathbf{P}(\mathbf{x}, t) = \int_0^t \xi_{\alpha, \beta}(t-s) \mathbf{E}(\mathbf{x}, s) ds, \quad \forall (\mathbf{x}, t) \in \Omega \times (0, T]. \quad (2.2)$$

Here $\xi_{\alpha, \beta}$ is the time-domain susceptibility kernel which involves the inverse Laplace transform as follows

$$\xi_{\alpha, \beta}(t) := \mathcal{L}^{-1} \left[\frac{\epsilon_0(\epsilon_s - \epsilon_\infty)}{(1 + (s\tau_0)^\alpha)^\beta} \right] (t), \quad (2.3)$$

and $\tau_0, \epsilon_s, \epsilon_\infty, \alpha, \beta$ are given in (1.1). As usual, \mathbf{E} is the electric field, \mathbf{H} is the magnetic field, and ϵ_0, μ_0 are the permittivity and permeability of the free space, respectively. The system (2.1)-(2.2) is supplemented with the perfect electrical conductor (PEC) condition

$$\mathbf{n} \times \mathbf{E} = \mathbf{0} \quad \text{at } \partial\Omega \times (0, T], \quad (2.4)$$

and the initial conditions

$$\mathbf{E}(\mathbf{x}, 0) = \mathbf{E}_0(\mathbf{x}), \quad \mathbf{H}(\mathbf{x}, 0) = \mathbf{H}_0(\mathbf{x}), \quad \mathbf{P}(\mathbf{x}, 0) = \mathbf{0} \quad \text{in } \Omega, \quad (2.5)$$

where the last condition is a direct consequence of the representation (2.2).

As the values of the parameters ϵ_0, μ_0 and τ_0 are excessively small (of order 10^{-12} , 10^{-7} and 10^{-12} , respectively), we find it is more desirable to rescale the model for both computational and analysis purposes. Indeed, the introduction of non-dimensional quantities can avoid dealing with excessively small or large numbers in finite-precision arithmetic (cf. [10, P. 294]).

Lemma 2.1. *Using the substitutions and change of variables*

$$\mathbf{E} \rightarrow \sqrt{\epsilon_0} \mathbf{E}, \quad \mathbf{P} \rightarrow \frac{1}{\sqrt{\epsilon_0}} \mathbf{P}, \quad \mathbf{H} \rightarrow \sqrt{\mu_0} \mathbf{H}, \quad t \rightarrow \frac{t}{\tau_0}, \quad \mathbf{x} \rightarrow \frac{\mathbf{x}}{c_0 \tau_0}, \quad c_0 := \frac{1}{\sqrt{\epsilon_0 \mu_0}}, \quad (2.6)$$

we can convert the system (2.1)-(2.5) into

$$\begin{cases} \epsilon_\infty \partial_t \mathbf{E} + \partial_t \mathbf{P} = \nabla \times \mathbf{H}, & \partial_t \mathbf{H} = -\nabla \times \mathbf{E} \quad \text{in } \Omega \times (0, T], \end{cases} \quad (2.7a)$$

$$\begin{cases} \mathbf{P}(\mathbf{x}, t) = \Delta \epsilon \int_0^t e^{\beta_{\alpha, \beta}(t-s)} \mathbf{E}(\mathbf{x}, s) ds \quad \text{in } \Omega \times (0, T], \end{cases} \quad (2.7b)$$

$$\begin{cases} \mathbf{E}(\mathbf{x}, 0) = \mathbf{E}_0(\mathbf{x}), \quad \mathbf{H}(\mathbf{x}, 0) = \mathbf{H}_0(\mathbf{x}), \quad \mathbf{P}(\mathbf{x}, 0) = \mathbf{0} \quad \text{in } \Omega, \end{cases} \quad (2.7c)$$

$$\begin{cases} \mathbf{n} \times \mathbf{E} = \mathbf{0} \quad \text{at } \partial\Omega \times (0, T], \end{cases} \quad (2.7d)$$

where $\Delta\epsilon := \epsilon_s - \epsilon_\infty$, and

$$e_{\rho,\mu}^\gamma(t; \sigma) = t^{\mu-1} E_{\rho,\mu}^\gamma(\sigma t^\rho), \quad E_{\rho,\mu}^\gamma(z) = \sum_{k=0}^{\infty} \frac{\Gamma(k+\gamma)}{\Gamma(k)\Gamma(\rho k + \mu)} \frac{z^k}{k!}, \quad (2.8)$$

i.e., the Mittag-Leffler (ML) function with three parameters (also known as the Prabhakar function, see, e.g., [17, 32]).

Proof. One verifies readily that with (2.6), the rescaled system (2.7) (except for (2.7b)) can be reduced from (2.1) and (2.4)-(2.5) directly.

Now, we consider the derivation of (2.7b). According to [17, (5.1.6), P. 98], we have

$$\mathcal{L}[e_{\rho,\mu}^\gamma(t; \sigma)](s) = \mathcal{L}[t^{\mu-1} E_{\rho,\mu}^\gamma(\sigma t^\rho)](s) = \frac{s^{-\mu}}{(1 - \sigma s^{-\rho})^\gamma} = \frac{s^{\rho\gamma-\mu}}{(s^\rho - \sigma)^\gamma} \quad \text{for } \rho, \mu > 0, \quad (2.9)$$

which, together with (2.3), leads to

$$\xi_{\alpha,\beta}(t) = \frac{\epsilon_0 \Delta\epsilon}{\tau_0^{\alpha\beta}} \mathcal{L}^{-1}[(s^\alpha + 1/\tau_0^\alpha)^{-\beta}](t) = \frac{\epsilon_0 \Delta\epsilon}{\tau_0^{\alpha\beta}} e_{\alpha,\alpha\beta}^\beta\left(t; -\frac{1}{\tau_0^\alpha}\right). \quad (2.10)$$

Then (2.2) can be written as

$$\mathbf{P}(\mathbf{x}, t) = \frac{\epsilon_0 \Delta\epsilon}{\tau_0^{\alpha\beta}} \int_0^t e_{\alpha,\alpha\beta}^\beta(t-s; -1/\tau_0^\alpha) \mathbf{E}(\mathbf{x}, s) ds.$$

With the substitution $s \rightarrow \frac{s}{\tau_0}$ and $t \rightarrow \frac{t}{\tau_0}$, we can obtain (2.7b) from the above. \square

Formally, the rescaled polarisation relation (2.7b) can be reformulated as a fractional “differential” form using the Prabhakar integrals/derivatives (cf. [14, 16]), which turns out to be important for the stability analysis of the re-scaled model (2.7).

Definition 2.1. (see [14, (B.19)-(B.23)] or [16, (5.3)-(5.10)]) *For a function $f(t) \in L^1(0, T)$, the Prabhakar integral of order $\alpha, \beta > 0$ and with the parameter $\varrho > 0$ can be defined by*

$$({}_0\mathcal{J}_t^\alpha + \varrho)^\beta f(t) = \int_0^t e_{\alpha,\alpha\beta}^\beta(t-s; -\varrho) f(s) ds, \quad t \in (0, T). \quad (2.11)$$

If, in addition, $0 < \alpha\beta < 1$, the left-inverse of the above integral operator is the special derivative

$$({}_0\mathcal{D}_t^\alpha + \varrho)^\beta f(t) = \frac{d}{dt} \int_0^t e_{\alpha,1-\alpha\beta}^{-\beta}(t-s; -\varrho) f(s) ds. \quad (2.12)$$

For an absolutely continuous function $f(t)$, the Caputo-type derivative as the counterpart of the above derivative operator can be defined as

$$({}_0\mathcal{D}_t^\alpha + \varrho)^\beta f(t) = ({}_0\mathcal{D}_t^\alpha + \varrho)^\beta (f(t) - f(0^+)) = \int_0^t e_{\alpha,1-\alpha\beta}^{-\beta}(t-s; -\varrho) f'(s) ds. \quad (2.13)$$

In view of (2.11), we can write (2.7b) as

$$\mathbf{P}(\mathbf{x}, t) = \Delta\epsilon ({}_0\mathcal{J}_t^\alpha + 1)^\beta \mathbf{E}(\mathbf{x}, t), \quad (2.14)$$

Taking the left-inverse operation (2.12) on both sides of (2.14), we obtain immediately from (2.13) that

$$({}_0\mathcal{D}_t^\alpha + 1)^\beta \mathbf{P}(\mathbf{x}, t) = ({}_0\mathcal{D}_t^\alpha + 1)^\beta \mathbf{P}(\mathbf{x}, t) = \Delta\epsilon \mathbf{E}(\mathbf{x}, t). \quad (2.15)$$

It is noteworthy that when $\beta = 1$ (i.e., the C-C model), the involved fractional derivatives simply become the usual fractional Riemann-Liouville derivative and Caputo derivative operators as in [30]. In fact, fractional ADE-based approaches for the C-C model are based upon such a formulation. However, for the general H-N model, we find the integral formulation (2.14) is more suitable for the implementation, but the formulation (2.15) is useful in the analysis.

Lemma 2.2. *If $0 < \alpha, \beta \leq 1$ and $\varrho > 0$, then the kernel $e_{\alpha, 1-\alpha\beta}^{-\beta}(t; -\varrho)$ in (2.12) and (2.15) is positive-definite in the sense that*

$$\int_0^T \phi(t) \int_0^t e_{\alpha, 1-\alpha\beta}^{-\beta}(t-s; -\varrho) \phi(s) \, ds \, dt \geq 0, \quad \forall \phi \in C[0, T].$$

Proof. According to [27, (1.2)], it suffices to show that the kernel function $\mathcal{K}(t) := e_{\alpha, 1-\alpha\beta}^{-\beta}(t; -\varrho)$ satisfies

$$\operatorname{Re}\{\mathcal{L}[\mathcal{K}(t)](i\omega)\} \geq 0, \quad \forall \omega > 0,$$

where $\operatorname{Re}\{u\}$ stands for the real part of u and i is the imaginary unit. Using (2.9) with $\gamma = -\beta, \rho = \alpha, \mu = 1 - \alpha\beta, \sigma = \varrho$ and $s = i\omega$, we find from direction calculation that

$$\begin{aligned} \mathcal{L}[\mathcal{K}(t)](i\omega) &= \frac{(i\omega)^{\alpha(-\beta)-(1-\alpha\beta)}}{((i\omega)^\alpha + \varrho)^{-\beta}} = \frac{(\varrho + (i\omega)^\alpha)^\beta}{i\omega} = -i\omega^{-1} \left(\varrho + \omega^\alpha \cos \frac{\pi\alpha}{2} + i\omega^\alpha \cos \frac{\pi\alpha}{2} \right)^\beta \\ &= -i\omega^{-1} r^\beta (\cos \beta\theta + i \sin \beta\theta) = \omega^{-1} r^\beta (\sin \beta\theta - i \cos \beta\theta), \end{aligned}$$

where

$$r = \sqrt{\varrho^2 + 2\omega^\alpha \cos \frac{\pi\alpha}{2} + \omega^{2\alpha}}, \quad \tan \theta = \frac{\omega^\alpha \sin \frac{\pi\alpha}{2}}{\varrho + \omega^\alpha \cos \frac{\pi\alpha}{2}}.$$

As the parameters $0 < \alpha, \beta \leq 1$ and $\varrho > 0$, it is evident that $\theta \in (0, \pi/2)$. Therefore,

$$\operatorname{Re}\{\mathcal{L}[\mathcal{K}(t)](i\omega)\} = \omega^{-1} r^\beta \sin \beta\theta \geq 0, \quad \forall \omega > 0,$$

which completes the proof. \square

With the aid of Lemma 2.2, we are able to show the following stability result for the H-N model (2.7), which implies its well-posedness.

Theorem 2.1. *If $\mathbf{E}_0, \mathbf{H}_0 \in \mathbf{L}^2(\Omega)$ in (2.7), then its solution $\mathbf{E}, \mathbf{H}, \mathbf{P} \in L^\infty(0, T; \mathbf{L}^2(\Omega))$ satisfying*

$$\mathcal{E}(t) := \epsilon_\infty \|\mathbf{E}(\cdot, t)\|^2 + \|\mathbf{H}(\cdot, t)\|^2 \leq \epsilon_\infty \|\mathbf{E}_0\|^2 + \|\mathbf{H}_0\|^2 := \mathcal{E}_0, \quad \forall t \in (0, T), \quad (2.16)$$

and

$$\|\mathbf{P}\|_{L^\infty(0, T; \mathbf{L}^2(\Omega))} \leq \Delta \epsilon B \|\mathbf{E}\|_{L^\infty(0, T; \mathbf{L}^2(\Omega))}, \quad (2.17)$$

where the constant B is given by

$$B = T^{\alpha\beta} \sum_{k=0}^{\infty} \frac{|(\beta)_k|}{\alpha(k+\beta)|\Gamma(\alpha k + \alpha\beta)|} \frac{T^{\alpha k}}{k!}.$$

Proof. Multiplying the first equation in (2.7a) by \mathbf{E} , and integrating the resulted equation by the Green's formula over Ω , we obtain that

$$\epsilon_\infty (\partial_t \mathbf{E}, \mathbf{E}) + (\partial_t \mathbf{P}, \mathbf{E}) - (\mathbf{H}, \nabla \times \mathbf{E}) = 0, \quad (2.18)$$

where we used the boundary condition (2.7d). Similarly, we derive from the second equation in (2.7a) that

$$(\partial_t \mathbf{H}, \mathbf{H}) + (\nabla \times \mathbf{E}, \mathbf{H}) = 0. \quad (2.19)$$

As a direct consequence of (2.18)-(2.19), we have

$$\epsilon_\infty (\partial_t \mathbf{E}, \mathbf{E}) + (\partial_t \mathbf{H}, \mathbf{H}) + (\partial_t \mathbf{P}, \mathbf{E}) = 0, \quad \text{i.e.,} \quad \frac{1}{2} \mathcal{E}'(t) = -(\partial_t \mathbf{P}, \mathbf{E}).$$

In view of (2.15), we eliminate \mathbf{E} and integrate the resulted equation with respect to t over $(0, T)$, which, together with (2.13) and Lemma 2.2, leads to

$$\begin{aligned} \frac{1}{2}\mathcal{E}(T) - \frac{1}{2}\mathcal{E}_0 &= -\frac{1}{\Delta\epsilon} \int_0^T (\partial_t \mathbf{P}, {}^C_0\mathcal{D}_t^\alpha + 1)^\beta \mathbf{P} \, dt \\ &= -\frac{1}{\Delta\epsilon} \int_0^T \int_0^t e_{\alpha, 1-\alpha\beta}^{-\beta}(t-s; -1) (\partial_t \mathbf{P}, \partial_s \mathbf{P}) \, ds \, dt \leq 0, \end{aligned}$$

where we recall that $\Delta\epsilon > 0$. This yields (2.16).

We now turn to (2.17). It is clear that by (2.7b),

$$\begin{aligned} |\mathbf{P}(\mathbf{x}, t)| &\leq \Delta\epsilon \int_0^t |e_{\alpha, \alpha\beta}^\beta(t-s; -1) \mathbf{E}(\mathbf{x}, s)| \, ds \leq \Delta\epsilon \sup_{0 \leq s \leq t} |\mathbf{E}(\mathbf{x}, s)| \int_0^t |e_{\alpha, \alpha\beta}^\beta(t-s; -1)| \, ds \\ &\leq \Delta\epsilon \sup_{0 \leq s \leq t} |\mathbf{E}(\mathbf{x}, s)| \int_0^T |e_{\alpha, \alpha\beta}^\beta(u; -1)| \, du. \end{aligned}$$

We derive from (2.8) and direct calculation that

$$\int_0^T |e_{\alpha, \alpha\beta}^\beta(u; -1)| \, du = \int_0^T u^{\alpha\beta-1} |E_{\alpha, \alpha\beta}^\beta(u; -1)| \, du \leq \sum_{k=0}^{\infty} \frac{|(\beta)_k|}{\Gamma(\alpha k + \alpha\beta)} \frac{1}{k!} \int_0^T u^{\alpha k + \alpha\beta-1} \, du := B,$$

where the quantity B is finite (cf. [23, Theorem 5] for the estimates of generalised ML functions). Thus, we obtain the first inequality but wish to show the second inequality below

$$|\mathbf{P}(\mathbf{x}, t)|^2 \leq (\Delta\epsilon)^2 B^2 \left(\sup_{0 \leq s \leq t} |\mathbf{E}(\mathbf{x}, s)| \right)^2 \leq (\Delta\epsilon)^2 B^2 \sup_{0 \leq s \leq t} |\mathbf{E}(\mathbf{x}, s)|^2. \quad (2.20)$$

Let $s_0 \in [0, t]$ satisfy

$$|\mathbf{E}(\mathbf{x}, s_0)|^2 = \sup_{0 \leq s \leq t} |\mathbf{E}(\mathbf{x}, s)|^2, \quad \text{so } |\mathbf{E}(\mathbf{x}, s_0)| \geq |\mathbf{E}(\mathbf{x}, s)|, \quad \forall s \in [0, t],$$

which implies

$$|\mathbf{E}(\mathbf{x}, s_0)|^2 \geq \left(\sup_{0 \leq s \leq t} |\mathbf{E}(\mathbf{x}, s)| \right)^2,$$

leading to the second inequality in (2.20). Therefore, we have

$$\sup_{0 \leq s \leq t} |\mathbf{P}(\mathbf{x}, s)|^2 \leq (\Delta\epsilon)^2 B^2 \sup_{0 \leq s \leq t} |\mathbf{E}(\mathbf{x}, s)|^2, \quad \forall t \in (0, T].$$

Integrating this inequality over Ω , leads to (2.17). \square

3. ANALYSIS OF A SEMI-DISCRETE TIME-DISCRETISATION SCHEME

In this section, we propose a time-discretisation scheme for the H-N model (2.7), and conduct the stability and convergence analysis.

3.1. Time discretisation. We start with a weak form of (2.7). Multiplying the three equations in (2.7) by the respective test functions, integrating over Ω and using the boundary conditions, we arrive at the weak form: find $\mathbf{E} \in C(0, T; H_0(\text{curl}, \Omega)) \cap C^1(0, T; \mathbf{L}^2(\Omega))$, $\mathbf{H} \in C(0, T; \mathbf{L}^2(\Omega)) \cap C^1(0, T; \mathbf{L}^2(\Omega))$ and $\mathbf{P} \in C^1(0, T; \mathbf{L}^2(\Omega))$ such that

$$\epsilon_\infty (\partial_t \mathbf{E}, \phi) + (\partial_t \mathbf{P}, \phi) - (\mathbf{H}, \nabla \times \phi) = 0, \quad \forall \phi \in H_0(\text{curl}, \Omega), \quad (3.1a)$$

$$(\partial_t \mathbf{H}, \psi) + (\nabla \times \mathbf{E}, \psi) = 0, \quad \forall \psi \in \mathbf{L}^2(\Omega), \quad (3.1b)$$

$$(\mathbf{P}, \varphi) = \Delta\epsilon \int_0^t e_{\alpha, \alpha\beta}^\beta(t-s; -1) (\mathbf{E}(\cdot, s), \varphi) \, ds, \quad \forall \varphi \in \mathbf{L}^2(\Omega). \quad (3.1c)$$

We partition the time interval $[0, T]$, and denote

$$t_k = k\Delta t, \quad k = 0, 1, \dots, N_t, \quad \Delta t = [T/N_t]; \quad \delta_t u^k = \frac{u^k - u^{k-1}}{\Delta t},$$

where u^k stands for the approximation of u at time t_k .

We first consider the time discretisation of (2.7b), and employ the piecewise constant approximation $I_{\Delta t} \mathbf{E}$ of \mathbf{E} :

$$\begin{aligned} \mathbf{P}(\mathbf{x}, t_k) &= \Delta \epsilon \int_0^{t_k} e_{\alpha, \alpha\beta}^\beta(t_k - s; -1) I_{\Delta t} \mathbf{E}(\mathbf{x}, s) \, ds + \Delta \epsilon \mathbf{R}_0^k(\mathbf{x}) \\ &= \Delta \epsilon \sum_{j=1}^k \left(\int_{t_{j-1}}^{t_j} e_{\alpha, \alpha\beta}^\beta(t_k - s; -1) \, ds \right) \mathbf{E}(\mathbf{x}, t_j) + \Delta \epsilon \mathbf{R}_0^k(\mathbf{x}) \\ &= \Delta \epsilon \sum_{j=1}^k \varpi_{k-j}^{(\alpha, \beta)} \mathbf{E}(\mathbf{x}, t_j) + \Delta \epsilon \mathbf{R}_0^k(\mathbf{x}), \quad k \geq 1, \end{aligned} \quad (3.2)$$

where the residual and the weights are given by

$$\begin{aligned} \mathbf{R}_0^k(\mathbf{x}) &:= \int_0^{t_k} e_{\alpha, \alpha\beta}^\beta(t_k - s; -1) (\mathbf{E}(\mathbf{x}, s) - I_{\Delta t} \mathbf{E}(\mathbf{x}, s)) \, ds \\ &= \sum_{j=1}^k \int_{t_{j-1}}^{t_j} e_{\alpha, \alpha\beta}^\beta(t_k - s; -1) (\mathbf{E}(\mathbf{x}, s) - \mathbf{E}(\mathbf{x}, t_j)) \, ds, \end{aligned} \quad (3.3)$$

and

$$\varpi_{k-j}^{(\alpha, \beta)} := \int_{t_{j-1}}^{t_j} e_{\alpha, \alpha\beta}^\beta(t_k - s; -1) \, ds = \int_{(k-j)\Delta t}^{(k-j+1)\Delta t} e_{\alpha, \alpha\beta}^\beta(s; -1) \, ds, \quad (3.4)$$

respectively. Recall the property (cf. [15, (4)-(5)] or [17, (5.1.15), (5.1.19)]):

$$\int_0^z e_{\rho, \mu}^\gamma(s; \sigma) \, ds = e_{\rho, \mu+1}^\gamma(z; \sigma), \quad \forall \rho, \mu > 0. \quad (3.5)$$

Then we can express the weights as

$$\varpi_{k-j}^{(\alpha, \beta)} = e_{\alpha, \alpha\beta+1}^\beta((k-j+1)\Delta t; -1) - e_{\alpha, \alpha\beta+1}^\beta((k-j)\Delta t; -1), \quad 1 \leq j \leq k. \quad (3.6)$$

Note that we can compute them accurately by using the codes in [13] for the ML functions.

Lemma 3.1. (see [32, p.9]). *For all $\rho > 0$ and real γ, μ , the Mittag-Leffler function with three parameters $E_{\rho, \mu}^\gamma(-z)$ is bounded in a finite interval.*

We have the following important property of the weights in (3.6).

Lemma 3.2. *For $0 < \alpha < 1, 0 < \beta \leq 1$, and $1 \leq k \leq N_t$, the weights $\{\varpi_{k-j}^{(\alpha, \beta)}\}_{j=1}^k$ satisfy*

$$0 \leq \varpi_{k-1}^{(\alpha, \beta)} \leq \varpi_{k-2}^{(\alpha, \beta)} \leq \dots \leq \varpi_1^{(\alpha, \beta)} \leq \varpi_0^{(\alpha, \beta)} = (\Delta t)^{\alpha\beta} E_{\alpha, \alpha\beta+1}^\beta(-(\Delta t)^\alpha),$$

and $\varpi_0^{(\alpha, \beta)}$ is finite.

Proof. Using the integral mean-value theorem, we find from (3.4) that

$$\varpi_{k-j}^{(\alpha, \beta)} = \int_{t_{j-1}}^{t_j} e_{\alpha, \alpha\beta}^\beta(t_k - s; -1) \, ds = \Delta t e_{\alpha, \alpha\beta}^\beta(t_k - \theta; -1), \quad \exists \theta \in (t_{j-1}, t_j), \quad 1 \leq j \leq k.$$

According to [17, (5.1.10)], we have that for all $\sigma, t > 0$, the function $e_{\rho, \mu}^\gamma(t; -\sigma) = t^{\mu-1} E_{\rho, \mu}^\gamma(-\sigma t^\rho)$ is completely monotonic, if only if $0 < \rho < \mu \leq 1$ and $0 < \gamma \leq \mu/\rho$. Based on [17, Definition 3.22]), a

function $f : (0, \infty) \rightarrow (-\infty, \infty)$ is called completely monotonic if it possesses derivatives $f^{(n)}(t)$ of any order $n = 0, 1, \dots$, and the derivatives are alternating in sign, i.e.,

$$(-1)^n f^{(n)}(t) \geq 0, \quad \forall t \in (0, \infty).$$

Consequently, $e_{\alpha, \alpha\beta}^\beta(z; -1)$ is completely monotonic for $0 < \alpha < 1, 0 < \beta \leq 1$, and $z > 0$, so it is nonnegative and decreasing. Therefore, the monotonicity of the discrete kernels and $\varpi_{k-1}^{(\alpha, \beta)} \geq 0$ ($1 \leq k \leq N_t$) are proved.

By virtue of (3.6), we have $\varpi_0^{(\alpha, \beta)} = (\Delta t)^{\alpha\beta} E_{\alpha, \alpha\beta+1}^\beta(-(\Delta t)^\alpha)$ which is finite due to Lemma 3.1. \square

Remark 3.1. In what follows, we shall not consider the D-C model (i.e., $\alpha = 1$). In fact, the computational codes for the ML functions in [13] excludes the case with $\alpha = 1$. In fact, the D-C model can be solved by a very different method which we plan to report in a separate future work.

Now we present the semi-discrete time-discretisation scheme for the H-N model (2.7): find $\mathbf{E}^k \in H_0(\text{curl}, \Omega) \cap \mathbf{L}^2(\Omega)$, $\mathbf{H}^k \in \mathbf{L}^2(\Omega)$ and $\mathbf{P}^k \in \mathbf{L}^2(\Omega)$ such that

$$\epsilon_\infty (\delta_t \mathbf{E}^k, \phi) + (\delta_t \mathbf{P}^k, \phi) - (\mathbf{H}^k, \nabla \times \phi) = 0, \quad \forall \phi \in H_0(\text{curl}, \Omega), \quad (3.7a)$$

$$(\delta_t \mathbf{H}^k, \psi) + (\nabla \times \mathbf{E}^k, \psi) = 0, \quad \forall \psi \in \mathbf{L}^2(\Omega), \quad (3.7b)$$

$$(\mathbf{P}^k, \varphi) = \Delta \epsilon \sum_{j=1}^k \varpi_{k-j}^{(\alpha, \beta)} (\mathbf{E}^j, \varphi), \quad \forall \varphi \in \mathbf{L}^2(\Omega), \quad (3.7c)$$

for $k = 1, 2, \dots, N_t$, where $\mathbf{E}^0 = \mathbf{E}_0(\mathbf{x})$, $\mathbf{H}^0 = \mathbf{H}_0(\mathbf{x})$ and $\mathbf{P}^0 = \mathbf{0}$.

3.2. Stability and discrete energy dissipation. In the convergence analysis, it is necessary to consider a more general setting:

$$\epsilon_\infty (\delta_t \mathbf{E}^k, \phi) + (\delta_t \mathbf{P}^k, \phi) - (\mathbf{H}^k, \nabla \times \phi) = (\mathbf{f}^k, \phi), \quad \forall \phi \in H_0(\text{curl}, \Omega), \quad (3.8a)$$

$$(\delta_t \mathbf{H}^k, \psi) + (\nabla \times \mathbf{E}^k, \psi) = (\mathbf{g}^k, \psi), \quad \forall \psi \in \mathbf{L}^2(\Omega), \quad (3.8b)$$

$$(\mathbf{P}^k, \varphi) = \Delta \epsilon \sum_{j=1}^k \varpi_{k-j}^{(\alpha, \beta)} (\mathbf{E}^j, \varphi) + \Delta \epsilon (\mathbf{h}^k, \varphi), \quad \forall \varphi \in \mathbf{L}^2(\Omega), \quad (3.8c)$$

where $\mathbf{E}^0 = \mathbf{E}_0(\mathbf{x})$, $\mathbf{H}^0 = \mathbf{H}_0(\mathbf{x})$ and $\mathbf{P}^0 = \mathbf{0}$. We shall see from the error equations (3.26)-(3.27) for convergence analysis that these non-homogeneous data will correspond to the time-discretisation errors of the fields.

Theorem 3.1. Let $\mathbf{E}^k, \mathbf{P}^k, \mathbf{H}^k$ be the solutions of (3.7) or (3.8), and define

$$\mathcal{E}^k := \epsilon_\infty \|\mathbf{E}^k\|^2 + \|\mathbf{H}^k\|^2 + \Delta \epsilon \sum_{j=1}^k \varpi_{k-j}^{(\alpha, \beta)} \|\mathbf{E}^j\|^2, \quad k \geq 1; \quad \mathcal{E}^0 := \epsilon_\infty \|\mathbf{E}^0\|^2 + \|\mathbf{H}^0\|^2. \quad (3.9)$$

Then the scheme (3.7) is unconditionally stable in the sense that for all $\Delta t > 0$,

$$\mathcal{E}^k \leq \mathcal{E}^{k-1} \leq \dots \leq \mathcal{E}^1 \leq \mathcal{E}^0. \quad (3.10)$$

For the scheme (3.8) with nonhomogeneous data, if $\varrho \Delta t < 1$ for some given positive constant $\varrho > 0$, and

$$\mathbf{Q}^k := \Delta t \sum_{j=1}^k (\|\mathbf{f}^j\|^2 + (\Delta \epsilon)^2 \|\delta_t \mathbf{h}^j\|^2 + \|\mathbf{g}^j\|^2) < \infty, \quad (3.11)$$

then we have

$$\mathcal{E}^k \leq \frac{1}{1 - \varrho \Delta t} \exp\left(\frac{\varrho t_{k-1}}{1 - \varrho \Delta t}\right) \left(\mathcal{E}^0 + \frac{1}{\varrho} \mathbf{Q}^k\right), \quad k \geq 1. \quad (3.12)$$

Proof. We first prove (3.12), and then (3.10) follows straightforwardly.

Taking $\phi = \Delta t \mathbf{E}^k$ in (3.8a) and $\psi = \Delta t \mathbf{H}^k$ in (3.8b), respectively, and adding two resulted equations together, we obtain

$$\begin{aligned} \epsilon_\infty (\mathbf{E}^k - \mathbf{E}^{k-1}, \mathbf{E}^k) + (\mathbf{H}^k - \mathbf{H}^{k-1}, \mathbf{H}^k) + (\mathbf{P}^k - \mathbf{P}^{k-1}, \mathbf{E}^k) \\ = \Delta t (\mathbf{f}^k, \mathbf{E}^k) + \Delta t (\mathbf{g}^k, \mathbf{H}^k). \end{aligned} \quad (3.13)$$

We eliminate \mathbf{P} from the above identity by using (3.8c) with $\varphi = \mathbf{E}^k$, so we can rewrite (3.13) as

$$\begin{aligned} \epsilon_\infty (\mathbf{E}^k, \mathbf{E}^k) + (\mathbf{H}^k, \mathbf{H}^k) + \Delta \epsilon \sum_{j=1}^k \varpi_{k-j}^{(\alpha, \beta)} (\mathbf{E}^j, \mathbf{E}^k) \\ = \epsilon_\infty (\mathbf{E}^{k-1}, \mathbf{E}^k) + (\mathbf{H}^{k-1}, \mathbf{H}^k) + \Delta \epsilon \sum_{j=1}^{k-1} \varpi_{k-1-j}^{(\alpha, \beta)} (\mathbf{E}^j, \mathbf{E}^k) \\ + \Delta t (\mathbf{f}^k + \Delta \epsilon \delta_t \mathbf{h}^k, \mathbf{E}^k) + \Delta t (\mathbf{g}^k, \mathbf{H}^k). \end{aligned} \quad (3.14)$$

Rearranging (3.14) yields

$$\begin{aligned} (\epsilon_\infty + \Delta \epsilon \varpi_0^{(\alpha, \beta)}) \|\mathbf{E}^k\|^2 + \|\mathbf{H}^k\|^2 \\ = \epsilon_\infty (\mathbf{E}^{k-1}, \mathbf{E}^k) + (\mathbf{H}^{k-1}, \mathbf{H}^k) + \Delta \epsilon \sum_{j=1}^{k-1} (\varpi_{k-1-j}^{(\alpha, \beta)} - \varpi_{k-j}^{(\alpha, \beta)}) (\mathbf{E}^j, \mathbf{E}^k) \\ + \Delta t (\mathbf{f}^k + \Delta \epsilon \delta_t \mathbf{h}^k, \mathbf{E}^k) + \Delta t (\mathbf{g}^k, \mathbf{H}^k). \end{aligned} \quad (3.15)$$

For $k \geq 2$, using the Cauchy-Schwarz inequality and Lemma 3.2, we obtain

$$\begin{aligned} (\epsilon_\infty + \Delta \epsilon \varpi_0^{(\alpha, \beta)}) \|\mathbf{E}^k\|^2 + \|\mathbf{H}^k\|^2 &\leq \frac{\epsilon_\infty}{2} (\|\mathbf{E}^k\|^2 + \|\mathbf{E}^{k-1}\|^2) + \frac{1}{2} (\|\mathbf{H}^k\|^2 + \|\mathbf{H}^{k-1}\|^2) \\ &+ \frac{\Delta \epsilon}{2} \sum_{j=1}^{k-1} (\varpi_{k-1-j}^{(\alpha, \beta)} - \varpi_{k-j}^{(\alpha, \beta)}) (\|\mathbf{E}^k\|^2 + \|\mathbf{E}^j\|^2) \\ &+ \frac{\varrho \Delta t}{2} (\|\mathbf{E}^k\|^2 + \|\mathbf{H}^k\|^2) + \frac{\Delta t}{2\varrho} (\|\mathbf{f}^k + \Delta \epsilon \delta_t \mathbf{h}^k\|^2 + \|\mathbf{g}^k\|^2), \end{aligned} \quad (3.16)$$

where $\varrho > 0$ is a constant independent of Δt and k . It is evident that

$$\sum_{j=1}^{k-1} (\varpi_{k-1-j}^{(\alpha, \beta)} - \varpi_{k-j}^{(\alpha, \beta)}) \|\mathbf{E}^k\|^2 = (\varpi_0^{(\alpha, \beta)} - \varpi_{k-1}^{(\alpha, \beta)}) \|\mathbf{E}^k\|^2. \quad (3.17)$$

Consequently, by (3.9), we find from (3.16)-(3.17) immediately that

$$\mathcal{E}^k - \varrho \Delta t (\|\mathbf{E}^k\|^2 + \|\mathbf{H}^k\|^2) \leq \mathcal{E}^{k-1} + \frac{\Delta t}{\varrho} (\|\mathbf{f}^k + \Delta \epsilon \delta_t \mathbf{h}^k\|^2 + \|\mathbf{g}^k\|^2), \quad (3.18)$$

which implies

$$(1 - \varrho \Delta t) \mathcal{E}^k \leq \mathcal{E}^{k-1} + \frac{\Delta t}{\varrho} (\|\mathbf{f}^k\|^2 + (\Delta \epsilon)^2 \|\delta_t \mathbf{h}^k\|^2 + \|\mathbf{g}^k\|^2). \quad (3.19)$$

In fact, (3.19) also holds for $k = 1$. Indeed, by (3.13) with $k = 1$, and understanding the summation $\sum_{n=1}^0 = 0$ in (3.14)-(3.17), we can get (3.19) with $k = 1$ readily.

For clarity, we set $k = j$ and rewrite (3.19) as

$$(1 - \varrho \Delta t) (\mathcal{E}^j - \mathcal{E}^{j-1}) \leq \varrho \Delta t \mathcal{E}^{j-1} + \frac{\Delta t}{\varrho} (\|\mathbf{f}^j\|^2 + (\Delta \epsilon)^2 \|\delta_t \mathbf{h}^j\|^2 + \|\mathbf{g}^j\|^2), \quad j \geq 1. \quad (3.20)$$

Summing it up for $1 \leq j \leq k$, we have that if $\varrho\Delta t < 1$,

$$\mathcal{E}^k \leq \frac{1}{1 - \varrho\Delta t} \left\{ \varrho\Delta t \sum_{j=1}^{k-1} \mathcal{E}^j + \mathcal{E}^0 + \frac{\Delta t}{\varrho} \sum_{j=1}^k (\|\mathbf{f}^j\|^2 + (\Delta\epsilon)^2 \|\delta_t \mathbf{h}^j\|^2 + \|\mathbf{g}^j\|^2) \right\}. \quad (3.21)$$

Using the discrete Grönwall's inequality (see, e.g., [33, Lemma 1.4.2]), we derive (3.12) directly.

We now turn to (3.7). In this case, we have $\mathbf{f}^k = \mathbf{g}^k = \mathbf{h}^k = \mathbf{0}$ in (3.13). Following the same lines as in the above derivations, we find readily that (3.18) becomes $\mathcal{E}^k \leq \mathcal{E}^{k-1}$, so the decay of the discrete energy in (3.10) holds. The proof is completed. \square

Remark 3.2. We can represent the constant in the bound (3.12) more explicitly so that it does not depend on Δt . For example, we take $\varrho = 1$ and assume that $1 - \Delta t \geq c_* > 0$, i.e., $\Delta t < 1 - c_*$. Then

$$\mathcal{E}^k \leq \frac{1}{c_*} \exp\left(\frac{t_{k-1}}{c_*}\right) (\mathcal{E}^0 + \mathbf{Q}^k), \quad k \geq 1. \quad (3.22)$$

With the aid of Theorem 3.1, we can further derive the following bound for \mathbf{P}^k in (3.7c).

Corollary 3.1. Let $\mathbf{E}^k, \mathbf{P}^k, \mathbf{H}^k$ be the solution of (3.7). Then we have

$$\|\mathbf{P}^k\| \leq (\Delta\epsilon e_{\alpha, \alpha\beta+1}^\beta(t_k; -1)) \max_{1 \leq j \leq k} \|\mathbf{E}^j\| \leq (\Delta\epsilon e_{\alpha, \alpha\beta+1}^\beta(t_k; -1)) \sqrt{\mathcal{E}^0}, \quad (3.23)$$

for $k \geq 1$, where $e_{\alpha, \alpha\beta+1}^\beta(t_k; -1)$ defined in (2.8) is finite for $0 < t_k \leq T$.

Proof. From (3.7c), we obtain

$$\|\mathbf{P}^k\|^2 = (\mathbf{P}^k, \mathbf{P}^k) = \Delta\epsilon \sum_{j=1}^k \varpi_{k-j}^{(\alpha, \beta)} (\mathbf{E}^j, \mathbf{P}^k) \leq \Delta\epsilon \sum_{j=1}^k \varpi_{k-j}^{(\alpha, \beta)} \|\mathbf{E}^j\| \|\mathbf{P}^k\|.$$

Thus, one has

$$\begin{aligned} \|\mathbf{P}^k\| &\leq \Delta\epsilon \sum_{j=1}^k \varpi_{k-j}^{(\alpha, \beta)} \|\mathbf{E}^j\| \leq \Delta\epsilon \left(\max_{1 \leq j \leq k} \|\mathbf{E}^j\| \right) \left(\sum_{j=1}^k \varpi_{k-j}^{(\alpha, \beta)} \right) \\ &\leq \Delta\epsilon t_k^{\alpha\beta} E_{\alpha, \alpha\beta+1}^\beta(-t_k^\alpha) \left(\max_{1 \leq j \leq k} \|\mathbf{E}^j\| \right), \end{aligned} \quad (3.24)$$

where we used (3.6) and Lemma 3.1 to arrive at

$$\sum_{j=1}^k \varpi_{k-j}^{(\alpha, \beta)} = e_{\alpha, \alpha\beta+1}^\beta(t_k; -1) - e_{\alpha, \alpha\beta+1}^\beta(0; -1) = t_k^{\alpha\beta} E_{\alpha, \alpha\beta+1}^\beta(-t_k^\alpha) = e_{\alpha, \alpha\beta+1}^\beta(t_k; -1). \quad (3.25)$$

Then we obtain the second inequality in (3.23) from (3.10) immediately. The proof is completed. \square

Remark 3.3. For the C-C model (i.e., $\beta = 1$), the energy dissipation was proved by Li et al. [24], where the equation of the induced polarization and electric field was formulated as the Caputo fractional differential form (see (2.15) with $\beta = 1$). However, it appeared nontrivial to show the strong energy dissipation and stability similar to (3.10), as the bound therein contained a constant $C > 1$ between k th and $(k-1)$ th steps (see [24, Theorem 3.1]). Though our result does not resolve this deficiency, as we work with the integral formulation of the induced polarization and electric field, and the discretisation schemes are different, we believe our argument can shed light on the analysis of the scheme based on the fractional differential form. \square

3.3. Convergence analysis. Next, we carry out the convergence analysis of the semi-discrete scheme (3.7). Denote $\varepsilon_1^k = \mathbf{E}^k - \mathbf{E}(t_k)$, $\varepsilon_2^k = \mathbf{H}^k - \mathbf{H}(t_k)$, and $\varepsilon_3^k = \mathbf{P}^k - \mathbf{P}(t_k)$. Then we can derive the following error equations from subtracting (3.1) from (3.7):

$$\epsilon_\infty (\delta_t \varepsilon_1^k, \phi) + (\delta_t \varepsilon_3^k, \phi) - (\varepsilon_2^k, \nabla \times \phi) = (\mathbf{R}_1^k, \phi), \quad \forall \phi \in H_0(\text{curl}, \Omega), \quad (3.26a)$$

$$(\delta_t \varepsilon_2^k, \psi) + (\nabla \times \varepsilon_1^k, \psi) = (\mathbf{R}_2^k, \psi), \quad \forall \psi \in \mathbf{L}^2(\Omega), \quad (3.26b)$$

$$(\varepsilon_3^k, \varphi) = \Delta \epsilon \sum_{j=1}^k \varpi_{k-j}^{(\alpha, \beta)} (\varepsilon_1^j, \varphi) - \Delta \epsilon (\mathbf{R}_0^k, \varphi), \quad \forall \varphi \in \mathbf{L}^2(\Omega), \quad (3.26c)$$

for $k = 1, 2, \dots, N_t$, where \mathbf{R}_0^k is defined in (3.3) and

$$\begin{aligned} \mathbf{R}_1^k(\mathbf{x}) &= \epsilon_\infty (\partial_t \mathbf{E}(\mathbf{x}, t_k) - \delta_t \mathbf{E}(\mathbf{x}, t_k)) + \partial_t \mathbf{P}(\mathbf{x}, t_k) - \delta_t \mathbf{P}(\mathbf{x}, t_k), \\ \mathbf{R}_2^k(\mathbf{x}) &= \partial_t \mathbf{H}(\mathbf{x}, t_k) - \delta_t \mathbf{H}(\mathbf{x}, t_k). \end{aligned} \quad (3.27)$$

Now, we can present the following convergence result for the semi-discrete scheme. Before the proof, we first give the following lemma.

Lemma 3.3. *If $\mathbf{E}, \mathbf{P}, \mathbf{H} \in H^2(0, T; \mathbf{L}^2(\Omega))$ and $k \geq 1$, then we have*

$$\|\mathbf{R}_1^k\| \leq C \Delta t (\|\mathbf{E}\|_{H^2(0, T; \mathbf{L}^2(\Omega))} + \|\mathbf{P}\|_{H^2(0, T; \mathbf{L}^2(\Omega))}); \quad \|\mathbf{R}_2^k\| \leq C \Delta t \|\mathbf{H}\|_{H^2(0, T; \mathbf{L}^2(\Omega))}, \quad (3.28)$$

and

$$\|\mathbf{R}_0^k\| \leq C \Delta t \|\mathbf{E}\|_{H^1(0, T; \mathbf{L}^2(\Omega))}, \quad \|\delta_t \mathbf{R}_0^k\| \leq C \Delta t \|\mathbf{E}\|_{H^2(0, T; \mathbf{L}^2(\Omega))}, \quad (3.29)$$

where C is a generic positive constant independent of Δt and any field but depending on t_{k-1} .

Proof. From (3.27), we can obtain readily the estimates (3.28) using the standard finite difference analysis for $1 \leq k \leq N_t$.

We now derive (3.29). Denote $\mathbf{r}^k = \mathbf{E}(\mathbf{x}, t) - \mathbf{E}(\mathbf{x}, t_k)$, $t \in (t_{k-1}, t_k)$. Then by (3.3), (3.5) and the completely monotonicity of $e_{\alpha, \alpha\beta}^\beta(z; -(\Delta t)^\alpha)$ ($0 < \alpha < 1, 0 < \beta \leq 1, z > 0$) (see [17, (5.1.10)]), we have

$$\|\mathbf{R}_0^k\| \leq \Delta t \|\mathbf{E}\|_{H^1(0, T; \mathbf{L}^2(\Omega))} \int_0^{t_j} e_{\alpha, \alpha\beta}^\beta(t_j - s; -1) ds = \Delta t e_{\alpha, \alpha\beta+1}^\beta(t_j; -1) \|\mathbf{E}\|_{H^1(0, T; \mathbf{L}^2(\Omega))},$$

and

$$\begin{aligned} \|\delta_t \mathbf{R}_0^k\| &= \frac{1}{\Delta t} \left\| \sum_{j=1}^k \int_{t_{j-1}}^{t_j} e_{\alpha, \alpha\beta}^\beta(t_k - s; -1) \mathbf{r}^j(s) ds - \sum_{j=1}^{k-1} \int_{t_{j-1}}^{t_j} e_{\alpha, \alpha\beta}^\beta(t_{k-1} - s; -1) \mathbf{r}^j(s) ds \right\| \\ &\leq \frac{1}{\Delta t} \left\| \sum_{j=1}^{k-1} \int_{t_{j-1}}^{t_j} e_{\alpha, \alpha\beta}^\beta(t_{k-1} - s; -1) [\mathbf{r}^j(s + \Delta t) - \mathbf{r}^j(s)] ds \right\| + \frac{1}{\Delta t} \left\| \int_0^{t_1} e_{\alpha, \alpha\beta}^\beta(t_k - s; -1) \mathbf{r}^1(s) ds \right\| \\ &\leq \frac{1}{\Delta t} \left(C(\Delta t)^2 \|\mathbf{E}\|_{H^2(0, T; \mathbf{L}^2(\Omega))} \int_0^{t_{k-1}} e_{\alpha, \alpha\beta}^\beta(t_{k-1} - s; -1) ds \right. \\ &\quad \left. + C \Delta t \|\mathbf{E}\|_{H^1(0, T; \mathbf{L}^2(\Omega))} \int_0^{\Delta t} e_{\alpha, \alpha\beta}^\beta(t_k - s; -1) ds \right) \\ &\leq C \Delta t \|\mathbf{E}\|_{H^2(0, T; \mathbf{L}^2(\Omega))} \int_0^{t_{k-1}} e_{\alpha, \alpha\beta}^\beta(t_{k-1} - s; -1) ds + C e_{\alpha, \alpha\beta}^\beta(t_{k-1}; -1) \|\mathbf{E}\|_{H^1(0, T; \mathbf{L}^2(\Omega))} \int_0^{\Delta t} ds \\ &\leq C \Delta t (e_{\alpha, \alpha\beta+1}^\beta(t_{k-1}; -1) \|\mathbf{E}\|_{H^2(0, T; \mathbf{L}^2(\Omega))} + e_{\alpha, \alpha\beta}^\beta(t_{k-1}; -1) \|\mathbf{E}\|_{H^1(0, T; \mathbf{L}^2(\Omega))}). \end{aligned}$$

Then by Lemma 3.1, the proof is completed. \square

In light of Theorem 3.1 and Lemma 3.3, we obtain the following convergence result on the semi-discrete scheme (3.7).

Theorem 3.2. Let $\mathbf{E}(\mathbf{x}, t), \mathbf{P}(\mathbf{x}, t), \mathbf{H}(\mathbf{x}, t)$ be the solution of (2.7), and let $\mathbf{E}^k, \mathbf{P}^k, \mathbf{H}^k$ be the solution of (3.7). Assume that

$$\mathbf{E} \in H^2(0, T; H_0(\text{curl}, \Omega) \cap \mathbf{L}^2(\Omega)) \text{ and } \mathbf{P}, \mathbf{H} \in H^2(0, T; \mathbf{L}^2(\Omega)).$$

Then for $\Delta t < 1 - c^*$ for given constant $c^* \in (0, 1)$ as in Remark 3.2, we have the error estimate

$$\begin{aligned} & \|\mathbf{E}^k(\cdot) - \mathbf{E}(\cdot, t_k)\|^2 + \|\mathbf{H}^k(\cdot) - \mathbf{H}(\cdot, t_k)\|^2 + \|\mathbf{P}^k(\cdot) - \mathbf{P}(\cdot, t_k)\|^2 \\ & \leq C(\Delta t)^2 (\|\mathbf{E}\|_{H^2(0, T; \mathbf{L}^2(\Omega))}^2 + \|\mathbf{P}\|_{H^2(0, T; \mathbf{L}^2(\Omega))}^2 + \|\mathbf{H}\|_{H^2(0, T; \mathbf{L}^2(\Omega))}^2), \end{aligned} \quad (3.30)$$

where the constant C is inherited from Remark 3.2, Corollary 3.1 and Lemma 3.3.

Proof. Taking $\phi = \Delta t \boldsymbol{\varepsilon}_1^k$ in (3.26a), $\psi = \Delta t \boldsymbol{\varepsilon}_2^k$ in (3.26b), and $\varphi = \boldsymbol{\varepsilon}_3^k$ in (3.26c), and following the derivation of (3.15), we obtain

$$\begin{aligned} & (\epsilon_\infty + \Delta \epsilon \varpi_0^{(\alpha, \beta)}) \|\boldsymbol{\varepsilon}_1^k\|^2 + \|\boldsymbol{\varepsilon}_2^k\|^2 \\ & = \epsilon_\infty (\boldsymbol{\varepsilon}_1^{k-1}, \boldsymbol{\varepsilon}_1^k) + (\boldsymbol{\varepsilon}_2^{k-1}, \boldsymbol{\varepsilon}_2^k) + \Delta \epsilon \sum_{j=1}^{k-1} (\varpi_{k-1-j}^{(\alpha, \beta)} - \varpi_{k-j}^{(\alpha, \beta)}) (\boldsymbol{\varepsilon}_1^j, \boldsymbol{\varepsilon}_1^k) \\ & \quad + \Delta t (\mathbf{R}_1^k + \Delta \epsilon \delta_t \mathbf{R}_0^k, \boldsymbol{\varepsilon}_1^k) + \Delta t (\mathbf{R}_2^k, \boldsymbol{\varepsilon}_2^k). \end{aligned}$$

Then we can derive from Theorem 3.1 and Remark 3.2 that

$$\|\boldsymbol{\varepsilon}_1^k\|^2 + \|\boldsymbol{\varepsilon}_2^k\|^2 \leq C \Delta t \sum_{j=1}^k (\|\mathbf{R}_1^j\|^2 + (\Delta \epsilon)^2 \|\delta_t \mathbf{R}_0^j\|^2 + \|\mathbf{R}_2^j\|^2), \quad (3.31)$$

where we used the facts $\epsilon_\infty \geq 1$, $\Delta \epsilon \sum_{j=1}^k \varpi_{k-j}^{(\alpha, \beta)} \|\boldsymbol{\varepsilon}_1^j\|^2 \geq 0$, and $\boldsymbol{\varepsilon}_1^0 = \boldsymbol{\varepsilon}_2^0 = \mathbf{0}$.

Similar to the proof of Corollary 3.1, we find from (3.26c) that

$$\|\boldsymbol{\varepsilon}_3^k\| \leq \Delta \epsilon \sum_{j=1}^k \varpi_{k-j}^{(\alpha, \beta)} \|\boldsymbol{\varepsilon}_1^j\| + \Delta \epsilon \|\mathbf{R}_0^k\| \leq (\Delta \epsilon e_{\alpha, \alpha\beta+1}^\beta(t_k; -1)) \max_{1 \leq j \leq k} \|\boldsymbol{\varepsilon}_1^j\| + \Delta \epsilon \|\mathbf{R}_0^k\|. \quad (3.32)$$

Finally, applying Lemma 3.3 to (3.31)-(3.32), we arrive at the error estimate (3.30). \square

Remark 3.4. In principle, we can upgrade the first-order temporal scheme (3.7) to a second-order scheme. The essential component is to apply the piecewise linear approximation to (2.7b) that yields

$$\begin{aligned} \mathbf{P}(\mathbf{x}, t_k) & \approx \Delta \epsilon \sum_{j=1}^k \int_{t_{j-1}}^{t_j} e_{\alpha, \alpha\beta}^\beta(t_k - s; -1) \left\{ \frac{t_j - s}{t_j - t_{j-1}} \mathbf{E}^{j-1}(\mathbf{x}) + \frac{s - t_{j-1}}{t_j - t_{j-1}} \mathbf{E}^j(\mathbf{x}) \right\} ds \\ & := \Delta \epsilon \sum_{j=0}^k \rho_{k-j}^{(\alpha, \beta)} \mathbf{E}^j(\mathbf{x}), \quad k \geq 1, \end{aligned}$$

where the weights can be computed by

$$\rho_{k-j}^{(\alpha, \beta)} = \int_{t_{j-1}}^{t_j} e_{\alpha, \alpha\beta}^\beta(t_k - s; -1) \frac{s - t_{j-1}}{t_j - t_{j-1}} ds + \int_{t_j}^{t_{j+1}} e_{\alpha, \alpha\beta}^\beta(t_k - s; -1) \frac{t_{j+1} - s}{t_{j+1} - t_j} ds,$$

for $1 \leq j \leq k-1$, and $\{\rho_0^{(\alpha, \beta)}, \rho_k^{(\alpha, \beta)}\}$ have similar expressions. It is seen that the monotonicity of the weights in Lemma 3.2 has played a critical role in the analysis. However, it is still unknown if $\{\rho_{k-j}^{(\alpha, \beta)}\}$ enjoys the same property. In fact, we have observed from some numerical evidences that it is parametric dependent as this property is not true for all α, β .

4. IMPLEMENTATION AND NUMERICAL RESULTS

In this section, we follow the idea of [26, 45] to introduce a fast temporal convolution algorithm that can alleviate the history dependence of the temporal convolution in the scheme (3.7). It is noteworthy that the semi-discrete scheme and the analysis in Section 3, together with the fast algorithm to be described below, can be incorporated with various spatial discretisation. As an example, we demonstrate the full discretisation via a spectral-Galerkin method in two dimensions. We highlight that one can extend the framework to finite element methods in two or more dimensions.

4.1. Fast temporal convolution algorithm. Among many recent developments of fast algorithms in particular for fractional integral/derivatives, there are a few works on developing fast algorithms for the much more involved kernel function, i.e., the ML function with three parameters. This algorithm can incorporate into (3.7) with different spatial discretisations.

We summarise the algorithm as follows.

Step 1 Decompose (2.7b) as

$$\begin{aligned} \mathbf{P}(\mathbf{x}, t) &= \Delta\epsilon \int_{t-\Delta t}^t e_{\alpha, \alpha\beta}^\beta(t-s; -1) \mathbf{E}(\mathbf{x}, s) ds + \Delta\epsilon \int_0^{t-\Delta t} e_{\alpha, \alpha\beta}^\beta(t-s; -1) \mathbf{E}(\mathbf{x}, s) ds \\ &:= \mathcal{L}(\mathbf{E}; t) + \mathcal{H}(\mathbf{E}; t), \end{aligned} \quad (4.1)$$

where $\mathcal{L}(\mathbf{E}; t)$ and $\mathcal{H}(\mathbf{E}; t)$ are respectively the local and history parts. Corresponding to the discretisation in (3.2), we have

$$\mathcal{L}(\mathbf{E}; t_k) \approx \mathcal{L}(I_{\Delta t} \mathbf{E}; t_k) = \varpi_0^{(\alpha, \beta)} \mathbf{E}^k; \quad \mathcal{H}(\mathbf{E}; t_k) \approx \mathcal{H}(I_{\Delta t} \mathbf{E}; t_k).$$

We remark that the direct implementation based on the above requires $O(N_t)$ storage and $O(N_t^2)$ operations, which is computationally expensive for long time and multi-dimensional simulations. The essence of the fast algorithm is to further approximate the kernel function $e_{\alpha, \alpha\beta}^\beta(\cdot; -1)$ that allows for computing the history part in a recursive manner.

Step 2 Given an integer $B \geq 2$, let L be the smallest integer satisfying $t_k < 2B^L \Delta t$. For $\ell = 1, \dots, L-1$, we can determine the integer q_ℓ and $s_\ell = q_\ell B^\ell \Delta t$ such that

$$t_k - s_\ell \in I_\ell := [B^{\ell-1} \Delta t, (2B^\ell - 1) \Delta t].$$

As such, we have (see [26])

$$t_k - \Delta t = s_0 > s_1 > \dots > s_{L-1} > s_L = 0.$$

Step 3 Seek the approximation of $e_{\alpha, \alpha\beta}^\beta(t; -1)$ on I_ℓ by applying the trapezoidal rule to a parametrisation of the contour integral for the inverse Laplace transform:

$$\begin{aligned} e_{\alpha, \alpha\beta}^\beta(t; -1) &\approx \frac{1}{2\pi i} \int_{\Gamma_\ell} \mathcal{L}[e_{\alpha, \alpha\beta}^\beta(t; -1)](\lambda) e^{t\lambda} d\lambda = \frac{1}{2\pi i} \int_{\Gamma_\ell} \frac{e^{t\lambda}}{(\lambda^\alpha + 1)^\beta} d\lambda \\ &\approx \sum_{j=-N_{\text{col}}}^{N_{\text{col}}-1} \frac{\hat{\omega}_j^{(\ell)} e^{t\lambda_j^{(\ell)}}}{((\lambda_j^{(\ell)})^\alpha + 1)^\beta}, \end{aligned} \quad (4.2)$$

with a precision $\varepsilon_f > 0$ and a complex contour Γ_ℓ which can be suitably chosen following the ideas in [26, 13]. Here, $\hat{\omega}_j^{(\ell)}, \lambda_j^{(\ell)}$ are the weights and quadrature points for the contour Γ_ℓ . The number of quadrature points on Γ_ℓ , $2N_{\text{col}}$ is chosen independent of ℓ .

Step 4 Using (4.2), the history part $\mathcal{H}(I_{\Delta t} \mathbf{E}; t_k)$ can be approximated by

$$\mathcal{H}(I_{\Delta t} \mathbf{E}; t_k) = \text{Im} \left\{ \sum_{\ell=1}^L \sum_{j=-N_{\text{col}}}^{N_{\text{col}}-1} \frac{\hat{\omega}_j^{(\ell)} e^{(t_k - s_{\ell-1})\lambda_j^{(\ell)}}}{[(\lambda_j^{(\ell)})^\alpha + 1]^\beta} \mathbf{y}(s_{\ell-1}, \lambda_j^{(\ell)}) \right\},$$

where $\text{Im}\{u\}$ stands for the imaginary part of u , and

$$\mathbf{y}(s) = \mathbf{y}(s, s_\ell, \lambda_j^{(\ell)}) = \int_{s_\ell}^s e^{-(s-s_\ell)\lambda_j^{(\ell)}} I_{\Delta t} \mathbf{E}(s) ds$$

satisfies the following ODE

$$\mathbf{y}'(s) = \lambda_j^{(\ell)} \mathbf{y}(s) + I_{\Delta t} \mathbf{E}(s), \quad \mathbf{y}(s_\ell) = 0.$$

Remark 4.1. *This fast convolution algorithm has the same storage and computational cost as that in [26], i.e., it requires $O(\log N_t)$ storage and $O(N_t \log N_t)$ operations over N_t time steps, when only cost in time direction is considered. However, the direct implementation of the scheme (3.2) would require $O(N_t)$ storage and $O(N_t^2)$ operations, which is computationally expensive and forms a bottleneck for long time simulation. It is worthy noting that the kernel function in H-N model (see (2.8)) is much more complex than the kernel functions in [26, 45] and references therein, so how to develop a fast convolution algorithm for the H-N model is much more involved. We also point out that some different approaches were developed in [5, 44].*

4.2. Full discretisation of a two-dimensional H-N model. As an illustration of full-discrete scheme, we consider the spatial discretisation of the H-N model using the spectral-Galerkin method in two dimensions. More precisely, we consider (2.7) on the rectangular domain $\Omega = (a, b) \times (c, d)$ of the form:

$$\epsilon_\infty \partial_t \mathbf{E} + \partial_t \mathbf{P} = \text{curl } H, \quad \partial_t H = -\text{curl } \mathbf{E} \quad \text{in } \Omega \times (0, T], \quad (4.3a)$$

$$\mathbf{P}(x, y, t) = \Delta \epsilon \int_0^t e_{\alpha, \alpha\beta}^\beta(t-s; -1) \mathbf{E}(x, y, s) ds \quad \text{in } \Omega \times (0, T], \quad (4.3b)$$

$$\mathbf{E}(x, y, 0) = \mathbf{E}_0(x, y), \quad H(x, y, 0) = H_0(x, y), \quad \text{in } \Omega, \quad (4.3c)$$

$$E_x(x, c, t) = E_x(x, d, t) = E_y(a, y, t) = E_y(b, y, t) = 0 \quad \text{for } t \in (0, T], \quad (4.3d)$$

where $\mathbf{E} = (E_x, E_y)^T$ and $\mathbf{P} = (P_x, P_y)^T$ are vectors, but H is a scalar unknown. Recap on the two-types of curl operators:

$$\text{curl } H = (\partial_y H, -\partial_x H)^T, \quad \text{curl } \mathbf{E} = \partial_y E_x - \partial_x E_y.$$

Let \mathbb{P}_N be the space of the algebraic polynomials in one variable of degree not more than N , and let \mathbb{P}_N^0 be the subspace of \mathbb{P}_N , where each polynomial vanishes at the two end-points of the interval. We further denote $V_N = \mathbb{P}_N \times \mathbb{P}_N$, and define

$$\mathbf{V}_N^0 = \{(u, v)^T \in (V_N)^2 : u|_{y=c} = u|_{y=d} = 0, v|_{x=a} = v|_{x=b} = 0\}.$$

The full-discrete scheme for (2.1) is to find $\mathbf{E}_N^k, \mathbf{P}_N^k \in \mathbf{V}_N^0$ and $H_N^k \in V_N$ such that for $k \geq 1$,

$$\epsilon_\infty (\delta_t \mathbf{E}_N^k, \phi) + (\delta_t \mathbf{P}_N^k, \phi) = (\text{curl } H_N^k, \phi), \quad \forall \phi \in \mathbf{V}_N^0, \quad (4.4a)$$

$$(\delta_t H_N^k, \psi) = -(\text{curl } \mathbf{E}_N^k, \psi), \quad \forall \psi \in V_N, \quad (4.4b)$$

$$(\mathbf{P}_N^k, \varphi) = \Delta \epsilon \sum_{j=1}^k \varpi_{k-j}^{(\alpha, \beta)} (\mathbf{E}_N^j, \varphi), \quad \forall \varphi \in \mathbf{V}_N^0, \quad (4.4c)$$

where the initial values are

$$\mathbf{E}_N^0 = \mathcal{I}_N \mathbf{E}_0, \quad H_N^0 = \mathcal{I}_N H_0, \quad \mathbf{P}_N^0 = \mathbf{0}. \quad (4.5)$$

Here, $\mathcal{I}_N : C(\bar{\Omega}) \rightarrow V_N$ is the tensorial Legendre-Gauss-Lobatto (LGL) interpolation operator.

The stability and well-posedness of the scheme (4.4) is a direct consequence of Theorem 3.1.

Theorem 4.1. *The full-discrete scheme (4.4) is unconditionally stable in the sense that for all $\Delta t > 0$,*

$$\mathcal{E}_N^k \leq \mathcal{E}_N^{k-1} \leq \dots \leq \mathcal{E}_N^0, \quad k \geq 1,$$

where $\mathcal{E}_N^0 := \epsilon_\infty \|\mathbf{E}_N^0\|^2 + \|H_N^0\|^2$ and

$$\mathcal{E}_N^k := \epsilon_\infty \|\mathbf{E}_N^k\|^2 + \|H_N^k\|^2 + \Delta\epsilon \sum_{j=1}^k \varpi_{k-j}^{(\alpha,\beta)} \|\mathbf{E}_N^j\|^2, \quad k \geq 1.$$

Following the argument for proving Theorem 3.2, we can show the convergence. To this end, we sketch the proof with an emphasis on the estimation of spatial error.

Let $\mathbf{E}_* = (E_{x*}, E_{y*})^T \in \mathbf{V}_N^0$, $\mathbf{P}_* = (P_{x*}, P_{y*})^T \in \mathbf{V}_N^0$, and $H_* \in V_N$ be some suitable orthogonal projections to be specified later. We introduce

$$\begin{aligned} \mathbf{e}_1^k &= \mathbf{E}_N^k - \mathbf{E}_*, & e_2^k &= H_N^k - H_*, & \mathbf{e}_3^k &= \mathbf{P}_N^k - \mathbf{P}_*, \\ \boldsymbol{\eta}_1^k &= \mathbf{E}|_{t_k} - \mathbf{E}_*, & \eta_2^k &= H|_{t_k} - H_*, & \boldsymbol{\eta}_3^k &= \mathbf{P}|_{t_k} - \mathbf{P}_*. \end{aligned}$$

We infer from (2.1)-(4.4) the error equations:

$$\epsilon_\infty (\delta_t \mathbf{e}_1^k, \boldsymbol{\phi}) + (\delta_t \mathbf{e}_3^k, \boldsymbol{\phi}) - (e_2^k, \operatorname{curl} \boldsymbol{\phi}) = (\delta_t \boldsymbol{\eta}_3^k, \boldsymbol{\phi}) + (\mathbf{f}_1^k, \boldsymbol{\phi}), \quad (4.6a)$$

$$(\delta_t e_2^k, \psi) + (\operatorname{curl} \mathbf{e}_1^k, \psi) = (f_2^k, \psi), \quad (4.6b)$$

$$(\mathbf{e}_3^k, \boldsymbol{\varphi}) = \Delta\epsilon \sum_{j=1}^k \varpi_{k-j}^{(\alpha,\beta)} (\mathbf{e}_1^j, \boldsymbol{\varphi}) + (\boldsymbol{\eta}_3^k, \boldsymbol{\varphi}) - \Delta\epsilon (\mathbf{f}_3^k, \boldsymbol{\varphi}), \quad (4.6c)$$

where

$$\mathbf{f}_1^k := \mathbf{R}_1^k + \epsilon_\infty \delta_t \boldsymbol{\eta}_1^k - \operatorname{curl} \eta_2^k, \quad f_2^k := R_2^k + \delta_t \eta_2^k + \operatorname{curl} \boldsymbol{\eta}_1^k, \quad \mathbf{f}_3^k := \sum_{j=1}^k \varpi_{k-j}^{(\alpha,\beta)} \boldsymbol{\eta}_1^j + \mathbf{R}_0^k. \quad (4.7)$$

Here, \mathbf{R}_0^k , \mathbf{R}_1^k , and R_2^k are defined in (3.3) and (3.27) with reduction to the two-dimensional setting. Like (3.31), we can derive

$$\|\mathbf{e}_1^k\|^2 + \|e_2^k\|^2 \leq C \left(\|e_1^0\|^2 + \|e_2^0\|^2 + \Delta t \sum_{j=1}^k (\|\mathbf{f}_1^j\|^2 + (\Delta\epsilon)^2 \|\delta_t \mathbf{f}_3^j\|^2 + \|f_2^j\|^2) \right),$$

and similar to the proof of Corollary 3.1, we can obtain

$$\|\mathbf{e}_3^k\| \leq C \max_{1 \leq j \leq k} \|\mathbf{e}_1^j\| + \|\boldsymbol{\eta}_3^k\| + \Delta\epsilon \|\mathbf{f}_3^k\|.$$

Recall that Lemma 3.3 provides the error bounds of \mathbf{R}_0^k , \mathbf{R}_1^k , and R_2^k , so it suffices to estimate the errors involving $\boldsymbol{\eta}_1^k$, η_2^k and $\boldsymbol{\eta}_3^k$. We first deal with the summation in \mathbf{f}_3^k . Following the same lines as deriving the last estimate in Lemma 3.3, one has

$$\begin{aligned} \left\| \delta_t \left(\sum_{i=1}^j \varpi_{j-i}^{(\alpha,\beta)} \boldsymbol{\eta}_1^i \right) \right\| &= \frac{1}{\Delta t} \left\| \sum_{i=1}^j \varpi_{j-i}^{(\alpha,\beta)} \boldsymbol{\eta}_1^i - \sum_{i=1}^{j-1} \varpi_{j-1-i}^{(\alpha,\beta)} \boldsymbol{\eta}_1^i \right\| \\ &\leq \frac{1}{\Delta t} \left\| \sum_{i=1}^j \int_{t_{i-1}}^{t_i} e_{\alpha,\alpha\beta}^\beta(t_j - s; -1) \boldsymbol{\eta}_1^i \, ds - \sum_{i=1}^{j-1} \int_{t_{i-1}}^{t_i} e_{\alpha,\alpha\beta}^\beta(t_{j-1} - s; -1) \boldsymbol{\eta}_1^i \, ds \right\| \\ &= \frac{1}{\Delta t} \left\| \int_0^{t_1} e_{\alpha,\alpha\beta}^\beta(t_j - s; -1) \boldsymbol{\eta}_1^1 \, ds + \sum_{i=1}^{j-1} \int_{t_{i-1}}^{t_i} e_{\alpha,\alpha\beta}^\beta(t_{j-1} - s; -1) (\boldsymbol{\eta}_1^{i+1} - \boldsymbol{\eta}_1^i) \, ds \right\| \\ &\leq e_{\alpha,\alpha\beta}^\beta(t_{j-1}; -1) \|\boldsymbol{\eta}_1^1\| + \sum_{i=1}^{j-1} \int_{t_{i-1}}^{t_i} e_{\alpha,\alpha\beta}^\beta(t_{j-1} - s; -1) \|\delta_t \boldsymbol{\eta}_1^{i+1}\| \, ds. \end{aligned} \quad (4.8)$$

We proceed with introducing some orthogonal projections, and review the relevant approximation results in [41]. Let $\pi_{N,x}^1 : H^1(I_x) \rightarrow \mathbb{P}_N$ be the H^1 -orthogonal projection, and let $\pi_{N,x}^{1,0} : H_0^1(I_x) \rightarrow \mathbb{P}_N^0$ be the H_0^1 -orthogonal projection. Likewise, we can define the operators $\pi_{N,y}^1$ and $\pi_{N,y}^{1,0}$ on the interval I_y . Here we choose

$$\{E_{x*}; P_{x*}\} = (\pi_{N,x}^1 \circ \pi_{N,y}^{1,0})\{E_x; P_x\}, \quad \{E_{y*}; P_{y*}\} = (\pi_{N,x}^{1,0} \circ \pi_{N,x}^1)\{E_y; P_y\}, \quad H_* = (\pi_{N,x}^1 \circ \pi_{N,y}^1)H.$$

According to [41], we have

$$\|U_{x*} - U_x\|_{H^s(\Omega)} \leq cN^{s-r}\|U_x\|_{H^r(\Omega)}, \quad \|U_{y*} - U_y\|_{H^s(\Omega)} \leq cN^{s-r}\|U_y\|_{H^r(\Omega)}, \quad s = 0, 1, \quad r \geq 1, \quad (4.9)$$

and

$$\|U - \mathcal{I}_N U\| \leq cN^{-r}\|U\|_{H^r(\Omega)}, \quad r \geq 1. \quad (4.10)$$

Below, we shall set U to be the unknowns. Now we are in a position to give the error estimates involving η_1^k, η_2^k and η_3^k . From (4.9), we have

$$\|\eta_1^j\| \leq cN^{-r} (\|E_x(\cdot, t_j)\|_{H^r(\Omega)} + \|E_y(\cdot, t_j)\|_{H^r(\Omega)}) \leq cN^{-r}\|\mathbf{E}\|_{L^\infty(0,T;\mathbf{H}^r(\Omega))},$$

$$\|\eta_3^k\| \leq cN^{-r} (\|P_x(\cdot, t_k)\|_{H^r(\Omega)} + \|P_y(\cdot, t_k)\|_{H^r(\Omega)}) \leq cN^{-r}\|\mathbf{P}\|_{L^\infty(0,T;\mathbf{H}^r(\Omega))},$$

$$\|\delta_t \eta_1^k\| \leq c\|\partial_t \eta_1^k\| \leq cN^{-r} (\|\partial_t E_x(\cdot, t_k)\|_{H^r(\Omega)} + \|\partial_t E_y(\cdot, t_k)\|_{H^r(\Omega)}) \leq cN^{-r}\|\partial_t \mathbf{E}\|_{L^\infty(0,T;\mathbf{H}^r(\Omega))},$$

$$\begin{aligned} \|\text{curl } \eta_1^k\| &= \|\partial_y(E_x - E_{x*}) - \partial_x(E_y - E_{y*})\| \leq \|\partial_y(E_x - E_{x*})\| + \|\partial_x(E_y - E_{y*})\| \\ &\leq cN^{1-r} (\|E_x(\cdot, t_k)\|_{H^r(\Omega)} + \|E_y(\cdot, t_k)\|_{H^r(\Omega)}) \leq cN^{(1-r)}\|\mathbf{E}\|_{L^\infty(0,T;\mathbf{H}^r(\Omega))}, \end{aligned}$$

$$\|\delta_t \eta_2^k\| \leq c\|\partial_t \eta_2^k\| \leq cN^{-r}\|\partial_t H(\cdot, t_k)\|_{H^r(\Omega)} \leq cN^{-r}\|\partial_t H\|_{L^\infty(0,T;\mathbf{H}^r(\Omega))},$$

and

$$\|\text{curl } \eta_2^k\| = \|\partial_x \eta_2^k\| + \|\partial_y \eta_2^k\| \leq cN^{(1-r)}\|H^k\|_{H^r(\Omega)} \leq cN^{(1-r)}\|H\|_{L^\infty(0,T;\mathbf{H}^r(\Omega))}.$$

Using the triangular inequality and the approximation results (4.9)-(4.10), we obtain

$$\|\mathbf{e}_1^0\| \leq cN^{-r}\|\mathbf{E}_0\|_{\mathbf{H}^r(\Omega)}, \quad \|e_2^0\| \leq cN^{-r}\|H_0\|_{H^r(\Omega)},$$

for the initial errors. Collecting all the estimates above, and noting (4.8), we present the following convergence result.

Theorem 4.2. *Let $\mathbf{E}_N^k, \mathbf{P}_N^k, H_N^k$ be the solution of (4.4) that approximates the solution of (2.1). Assume*

$$E_x, P_x \in H^2(0, T; H^r(\Omega) \cap (H^1(I_x) \otimes H_0^1(I_y))), \quad E_y, P_y \in H^2(0, T; H^r(\Omega) \cap (H_0^1(I_x) \otimes H^1(I_y))),$$

and $H \in H^2(0, T; H^r(\Omega))$, then for $k \geq 1$,

$$\begin{aligned} &\|\mathbf{E}(\cdot, t_k) - \mathbf{E}_N^k\|^2 + \|H(\cdot, t_k) - H_N^k\|^2 + \|\mathbf{P}(\cdot, t_k) - \mathbf{P}_N^k\|^2 \\ &\leq C(\Delta t)^2 (\|\mathbf{E}\|_{H^2(0,T;\mathbf{L}^2(\Omega))}^2 + \|\mathbf{P}\|_{H^2(0,T;\mathbf{L}^2(\Omega))}^2 + \|H\|_{H^2(0,T;\mathbf{L}^2(\Omega))}^2) \\ &\quad + CN^{2(1-r)} (N^{-2}\|\mathbf{E}_0\|_{\mathbf{H}^r(\Omega)}^2 + N^{-2}\|H_0\|_{H^r(\Omega)}^2 + N^{-2}\|\partial_t \mathbf{E}\|_{L^\infty(0,T;\mathbf{H}^r(\Omega))}^2 + N^{-2}\|\partial_t H\|_{L^\infty(0,T;\mathbf{H}^r(\Omega))}^2 \\ &\quad + N^{-2}\|\mathbf{E}\|_{L^\infty(0,T;\mathbf{H}^r(\Omega))}^2 + N^{-2}\|\mathbf{P}\|_{L^\infty(0,T;\mathbf{H}^r(\Omega))}^2 + \|H\|_{L^\infty(0,T;\mathbf{H}^r(\Omega))}^2 + \|\mathbf{E}\|_{L^\infty(0,T;\mathbf{H}^r(\Omega))}^2), \end{aligned}$$

for a suitable Δt (see Theorem 3.1 and Remark 3.2). Here, C is a positive constant independent of $\Delta t, N$ and any function.

4.3. Numerical results. In this subsection, we provide ample numerical results to show the efficiency and accuracy of the proposed methods with a focus on the performance of the treatment in time discretisation.

4.3.1. *Accuracy and efficiency tests.* Consider the system (2.1) with the exact solution:

$$\begin{aligned} \mathbf{E}(x, y, t) &= \frac{t^4}{\Gamma(5)} \mathbf{w}(x, y), \quad \mathbf{P}(x, y, t) = \Delta\epsilon e_{\alpha, \alpha\beta+5}^\beta(t; -1) \mathbf{w}(x, y), \quad \mathbf{w}(x, y) = \begin{pmatrix} -\cos(\pi x) \\ \sin(\pi x) \end{pmatrix} \sin(\pi y), \\ H(x, y, t) &= \left(\frac{4\epsilon_\infty}{\pi\Gamma(5)} t^3 + \Delta\epsilon e_{\alpha, \alpha\beta+4}^\beta(t; -1) \right) \cos(\pi x) \cos(\pi y). \end{aligned}$$

As such, the second equation in (2.1) must have a source term

$$f(x, y, t) = \left(\frac{2\pi}{\Gamma(5)} t^4 + \frac{12\epsilon_\infty}{\pi\Gamma(5)} t^2 + \frac{\Delta\epsilon}{\pi} e_{\alpha, \alpha\beta+3}^\beta(t; -1) \right) \cos(\pi x) \cos(\pi y),$$

which one can verify by using the formulas in [23, (2.10) and (2.26)].

For notational simplicity, we denote by $U_{N,D}^k$ and $U_{N,F}^k$ the numerical solutions derived by the direct and fast algorithms at $t_k = k\Delta t$. Correspondingly, we denote the discrete L^2 -errors by $\text{ErrU}_F := \|U(\cdot, t_k) - U_{N,F}^k\|_N$ and $\text{ErrU}_{DF} := \|U_{N,D}^k - U_{N,F}^k\|_N$, respectively, where U can be \mathbf{E} , H or \mathbf{P} . In the following tests, we take $\Omega = (-1, 1)^2$ and $\epsilon_\infty = \Delta\epsilon = 1$.

TABLE 4.1. Errors and convergence rates of the fast temporal convolution algorithm.

τ	ErrE _F	Order	ErrH _F	Order	ErrP _F	Order	ErrE _{DF}	ErrH _{DF}	ErrP _{DF}
2^{-4}	6.4914e-03	-	2.0905e-03	-	6.1861e-03	-	2.8917e-16	1.4197e-16	2.5075e-16
2^{-6}	1.6836e-03	0.99	4.0510e-04	1.17	1.7062e-03	0.94	3.6776e-16	1.7787e-16	1.4391e-16
2^{-8}	4.1803e-04	1.01	8.3436e-05	1.13	4.5249e-04	0.96	2.7708e-16	4.3866e-16	5.4712e-17
2^{-10}	1.0307e-04	1.01	1.7985e-05	1.10	1.1771e-04	0.97	3.8889e-16	5.4694e-16	5.9642e-17
2^{-12}	2.5458e-05	1.01	4.0045e-06	1.08	3.0253e-05	0.98	1.6182e-15	1.8799e-16	1.3962e-15
2^{-14}	6.3060e-06	1.01	9.1495e-07	1.06	7.7104e-06	0.99	4.6538e-16	3.1352e-15	1.2561e-15

Firstly, in Table 4.1, we tabulate the discrete L^2 -errors between the exact and numerical solutions, together with convergence orders, obtained by the schemes with $\alpha = \beta = 0.5$ and $N = 50$ at $T = 1$. In the rightmost three columns, we list the errors between the numerical solutions by direct and fast algorithms (with $N_{\text{col}} = 30$), which are apparently negligible. We also observe that the first-order convergence as expected.

Secondly, we compare in Figure 4.1 the computational time in seconds against N_t between the direct and fast convolution algorithms with $\alpha = \beta = 0.5$, $N = 50$, $N_{\text{col}} = 30$ and with different Δt at $T = 1$. Note that the fast convolution algorithm requires $O(N_t \log N_t)$ operations over N_t time steps, while the direct algorithm requires $O(N_t^2)$ operations. As such, much saving can be achieved by using the fast convolution algorithm which is therefore necessary for long time simulation.

Finally, we depict in Figures 4.2-4.3 the convergence rates in both time and space with different parameters α, β . As expected, we observe from Figures 4.2 the first-order convergence order in time, while from Figures 4.3 the spectral accuracy in space (given the spatial smooth exact solution). Here, we understand $O(\Delta t) = 0.5\Delta t$. For the latter, we choose $\Delta t = 0.00001$ so that we can demonstrate the spatial errors. Indeed, the numerics confirm the convergence $O(\Delta t + e^{-cN})$ for some $c > 0$.

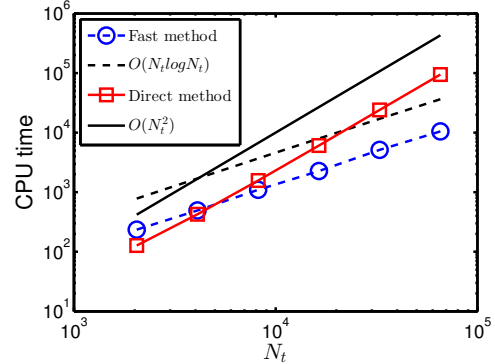
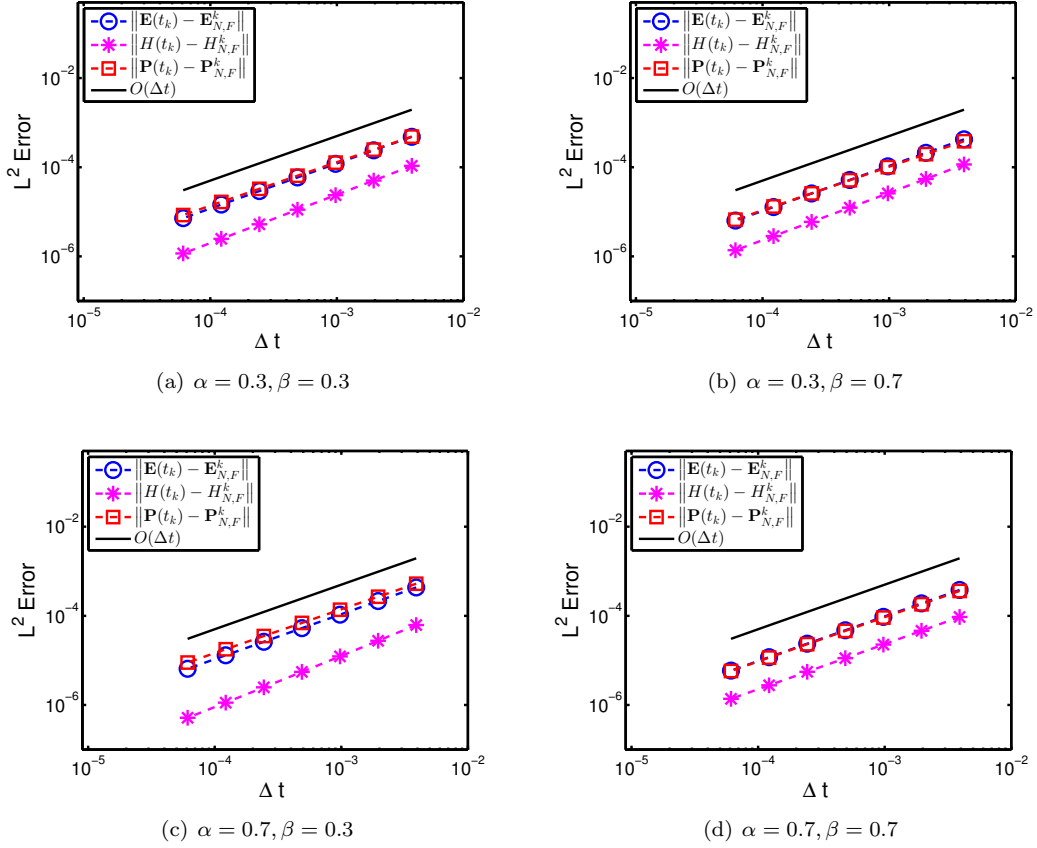
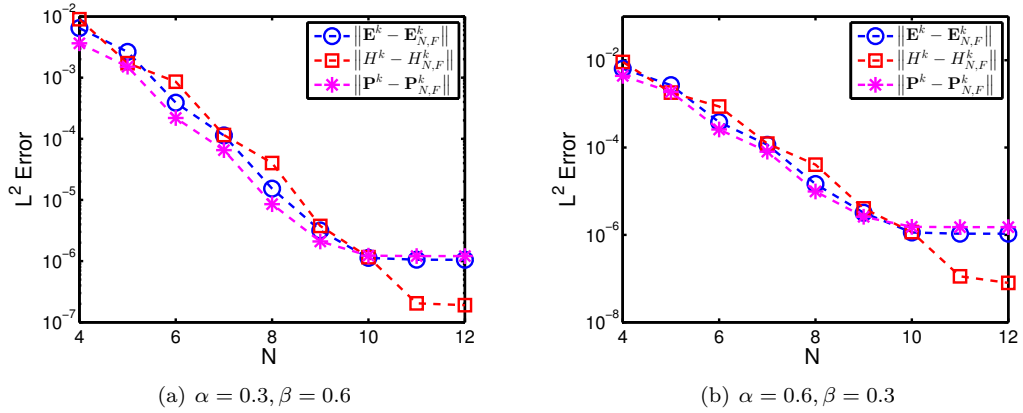


FIGURE 4.1. Direct versus fast algorithms

FIGURE 4.2. Convergence order in time with $N = 50$, $N_{\text{col}} = 30$ and different parameters α, β .FIGURE 4.3. Convergence behaviour in space for different parameters α, β .

4.3.2. *Discrete energy decay.* In order to illustrate the discrete energy dissipation shown in Theorem 4.1, we set the initial values to be

$$E_x(x, y, 0) = \frac{1}{\sqrt{2}} \cos(\pi x) \sin(\pi y), \quad E_y(x, y, 0) = -\frac{1}{\sqrt{2}} \sin(\pi x) \cos(\pi y), \quad H(x, y, 0) = 0.$$

Note that the system must be homogeneous to possess such a property (see (4.4)). As a result, we use sufficiently fine mesh grids to verify the accuracy and convergence order as observed previously. Here, we record in Figure 4.4 the evolution of the discrete energy \mathcal{E}_N^k obtained by the scheme with $\Delta t = 0.01$, $N = 50$ and $N_{\text{col}} = 30$ for some different parameters α, β . Indeed, these numerical evidences validate this behaviour. Interestingly, when it comes to the discrete analogue of the energy in Theorem 2.1: $\tilde{\mathcal{E}}_N^k := \epsilon_\infty \|\mathbf{E}_N^k\|^2 + \|\mathbf{H}_N^k\|^2$, we observe from Figure 4.5 that it fails to satisfy this decaying property. Indeed, as shown in Theorem 2.1, this energy at continuous level can only be controlled by the initial energy. In fact, a similar behaviour has been observed for the Cole-Cole model in [20].

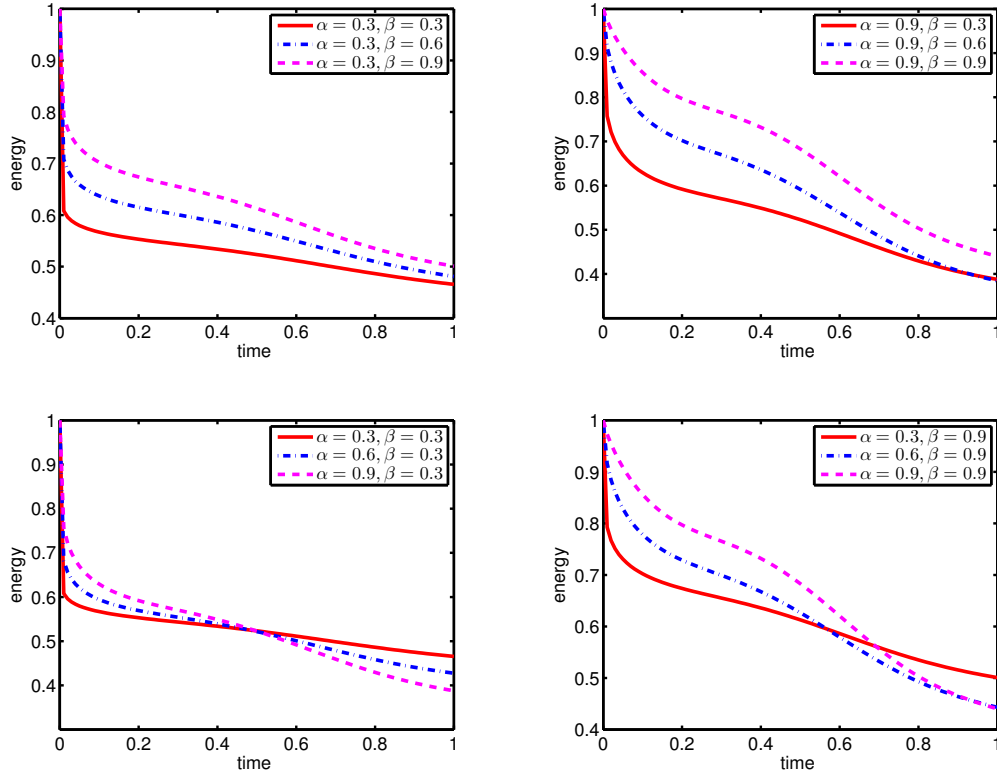
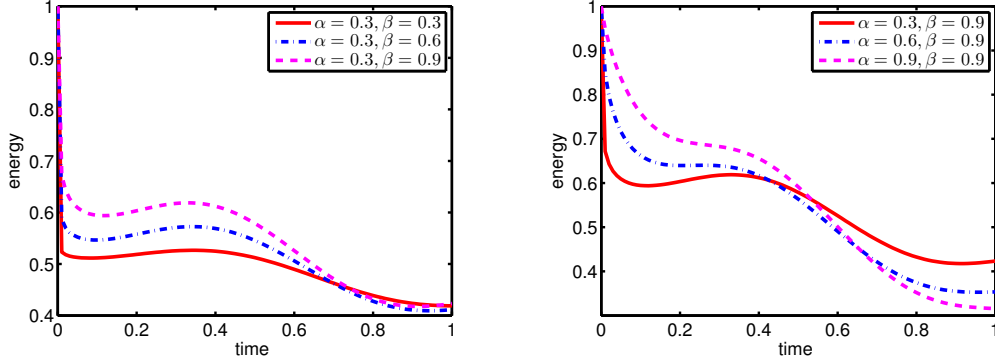


FIGURE 4.4. Evolution of the discrete energy \mathcal{E}_N^k with different α and β .

4.4. **Application: recovery of the relative permittivity, reflection coefficient and transfer function.** As already mentioned in the introductory section, the dispersive media in which the electromagnetic waves propagate, can be characterised by the relative permittivity:

$$\epsilon_r(\omega) = \epsilon_\infty + \frac{\epsilon_s - \epsilon_\infty}{(1 + (i\omega\tau_0)^\alpha)^\beta}, \quad (4.11)$$

FIGURE 4.5. Evolution of the discrete energy $\tilde{\mathcal{E}}_N^k$ with different α and β .

in terms of the frequency variable ω , for given ϵ_∞ , ϵ_s , τ_0 , α and β . It is of physical interest to study the associated reflection coefficient (cf. [2]) in magnitude:

$$|\mathcal{R}(\omega)| = |(1 - \sqrt{\epsilon_r(\omega)}) / (1 + \sqrt{\epsilon_r(\omega)})|. \quad (4.12)$$

Another closely related notion is the transfer function $T(d, \omega)$ (see, e.g., [35, 36, 37, 2]) given by

$$T(d, \omega) = e^{\Upsilon(\omega)d}, \quad \Upsilon(\omega) = -i\omega\sqrt{\epsilon_r(\omega)}/c_0 := \Upsilon_R(\omega) + i\Upsilon_I(\omega), \quad (4.13)$$

where $c_0 = 3.0 \times 10^8$ is the speed of light in free space. It describes the transfer rate of the electric field in frequency domain from the point \mathbf{x} to the point $\mathbf{x} + d$:

$$\widehat{\mathbf{E}}(\mathbf{x} + d, \omega) = T(d, \omega) \widehat{\mathbf{E}}(\mathbf{x}, \omega), \quad (4.14)$$

where $\widehat{\mathbf{E}}(\mathbf{x}, \omega)$ denotes the Fourier transform of the electric field $\mathbf{E}(\mathbf{x}, t)$.

In view of the above relations, one can compute $\mathbf{E}(\mathbf{x}, t)$ in time domain with fixed ϵ_∞ , ϵ_s , τ_0 , α and β by solving the Maxwell's system (2.1)-(2.5), and then transform the field to the frequency domain. From (4.14), we can compute the approximate transfer function $\tilde{T}(d, \omega)$ in ω (as the field \mathbf{E} is computed numerically), from which we can work out the approximate $\tilde{\epsilon}_r(\omega)$ and $|\tilde{\mathcal{R}}(\omega)|$ by using the relations (4.13) and (4.12), respectively. We are interested in fitting and recovering the analytic values of $\epsilon_r(\omega)$, $|\mathcal{R}(\omega)|$ and $T(d, \omega)$ (evaluated exactly by (4.11)-(4.13) with given ϵ_∞ , ϵ_s , τ_0 , α and β) by the corresponding approximate values as in [35, 36, 37, 2].

Similar to the setting in [2], we consider the Maxwell's system (2.1) in one spatial dimension with $z \in (a, b)$ and $t \in (0, T]$, but adding the source term $f(z, t) := E_{\text{inc}}(t)\chi_{z_*}(z)$ to the first equation of (2.1). Here, $E_{\text{inc}}(t)$ is a modulated Gaussian pulse (cf. [2]):

$$E_{\text{inc}}(t) = e^{-a_e^2(t-4/a_e)^2} \sin(2\pi f_e(t - 4/a_e))u(t), \quad (4.15)$$

where $a_e = 5 \times 10^9 \text{ s}^{-1}$, the central frequency $f_e = 6 \text{ GHz}$, and $u(t)$ is the unit step function, i.e., $u(t) = 1$ when $t \geq 0$ while $u(t) = 0$ when $t < 0$. Note that the energy of the pulse ranges from 0.1 GHz to 10 GHz. In the source term, $z_* \in (a, b)$ is the location where the pulse is excited, and $\chi_{z_*}(z) = 1$ at $z = z_*$, but it is equal to 0 elsewhere on (a, b) . It is noteworthy that the vector fields in the system (2.1) reduce to the scalar fields $E_x(z, t)$, $H_y(z, t)$ and $P_x(z, t)$ in one dimension.

For clarity, we sketch the algorithm as follows.

- (i) Solve the Maxwell's system for given ϵ_∞ , ϵ_s , τ_0 , α and β . Here, we adopt the finite-difference time-domain (FDTD) method to discretise the one dimensional system [2], but use the fractional integral formulation of the polarisation relation together with the aforementioned temporal discretisation, and fast convolution algorithm. With these, we can obtain the numerical approximation $E_{x,m}^k$ of $E_x(z, t)$ on the space-time grids: $t_k = k\Delta t$ and $z_m = a + m\Delta z$.
- (ii) Apply the discrete Fourier transform (cf. [11, P. 156]) to $\{E_{x,m_*}^k\}_{k=1}^{N_t}$ and $\{E_{x,m_*+l}^k\}_{k=1}^{N_t}$ (at the locations $z_* = z_{m_*}$ and $z = z_* + d$ with $d = l\Delta z$) from the time domain to the frequency domain that leads to $\{\hat{E}_{x,m_*}^{\omega_j}\}_{j=1}^{N_\omega}$ and $\{\hat{E}_{x,m_*+l}^{\omega_j}\}_{j=1}^{N_\omega}$. Then the approximate transfer function is

$$\tilde{T}(d, \omega_j) = \hat{E}_{x,m_*+l}^{\omega_j} / \hat{E}_{x,m_*}^{\omega_j}. \quad (4.16)$$

- (iii) Substitute (4.16) into (4.13) leading to the approximation:

$$\tilde{\Upsilon}_R(\omega_j) = \ln(|\hat{E}_{x,m_*+l}^{\omega_j} / \hat{E}_{x,m_*}^{\omega_j}|) / d, \quad \tilde{\Upsilon}_I(\omega_j) = (\arg\{\hat{E}_{x,m_*+l}^{\omega_j}\} - \arg\{\hat{E}_{x,m_*}^{\omega_j}\}) / d. \quad (4.17)$$

Accordingly, we derive from (4.13) and (4.17) the real and the imaginary part of the approximate relative permittivity:

$$\tilde{\epsilon}_r(\omega_j) = \tilde{\epsilon}'(\omega_j) - i\tilde{\epsilon}''(\omega_j) = -(c_0(\tilde{\Upsilon}_R(\omega_j) + i\tilde{\Upsilon}_I(\omega_j)) / \omega_j)^2,$$

and from (4.12) the approximate magnitude of the reflection coefficient:

$$|\tilde{\mathcal{R}}(\omega_j)| = \left| (1 - \sqrt{\tilde{\epsilon}_r(\omega_j)}) / (1 + \sqrt{\tilde{\epsilon}_r(\omega_j)}) \right|.$$

In the computation, we take $a = 0, b = 1.1$ m, $T = 5.304 \times 10^{-9}$ s, $\epsilon_s = 50$, $\epsilon_\infty = 2$, $\tau_0 = 1.53 \times 10^{-10}$ s, $\Delta t = 1.768 \times 10^{-12}$ s, $\Delta z = 1.1$ mm, $z_* = 0.55$ m, and sample $\{\omega_j\}_{j=1}^{N_\omega}$ in (0.1, 10) GHz as in [2]. In Figure 4.6, we plot the analytical magnitude of the reflection coefficient $|\mathcal{R}(\omega)|$ and approximate values against samples of $\{\omega_j\}$ with different α, β . In Figure 4.7, we show the analytical complex transfer function $T(d, \omega_j)$ and its approximation $\tilde{T}(d, \omega_j)$ with different α, β and d . We observe a better approximation than that in [2], which shows the advantage of our approach. In Figure 4.8, we depict the complex relative permittivity $\epsilon_r = \epsilon' - i\epsilon''$ and the approximate $\tilde{\epsilon}_r = \tilde{\epsilon}' - i\tilde{\epsilon}''$ with different α and β , which is not presented in [2]. Indeed, we observe a good agreement of the exact and numerical values.

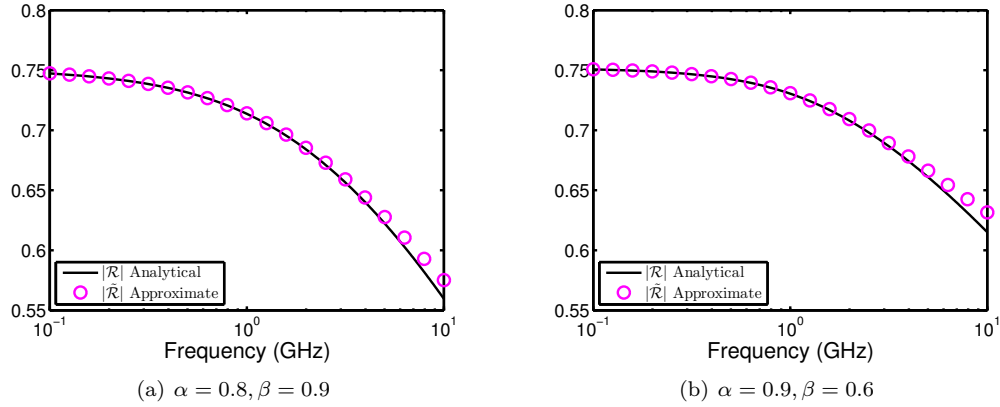


FIGURE 4.6. Real and imaginary part of the analytical magnitude of the reflection coefficient and the approximate value.

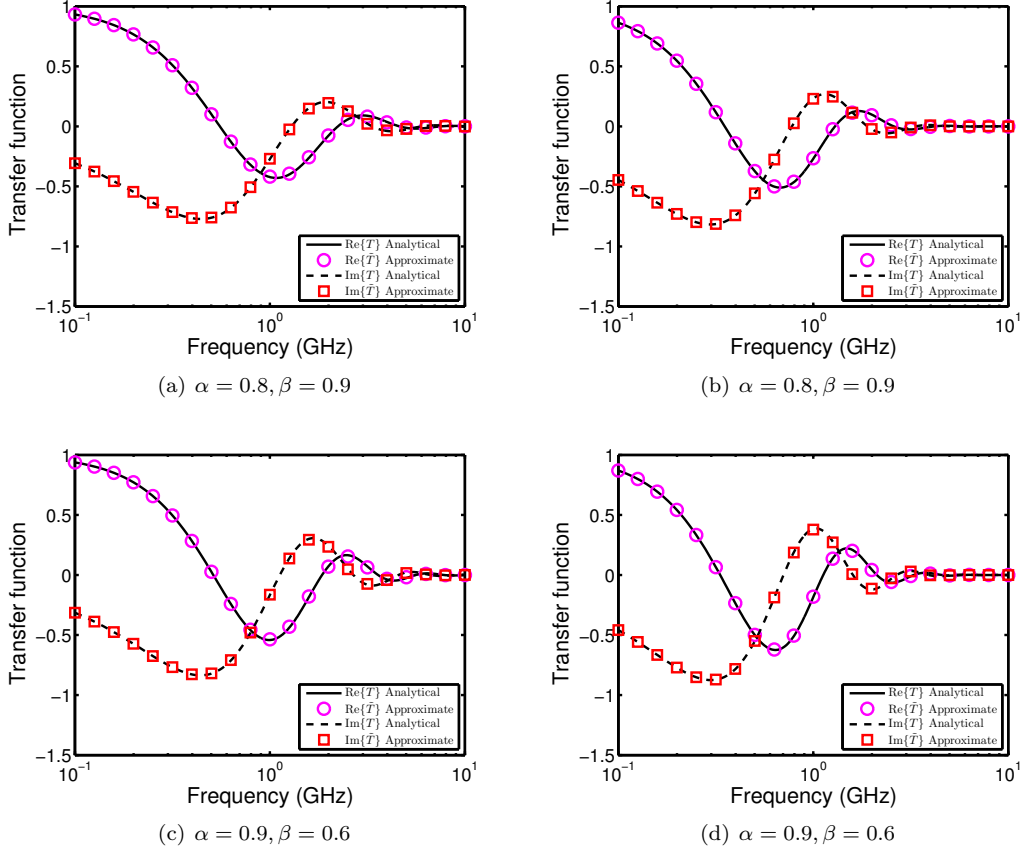


FIGURE 4.7. Real and imaginary part of the analytical complex transfer function and the approximate one of the H-N medium. (Left): $d = 20\Delta z$; (Right): $d = 30\Delta z$.

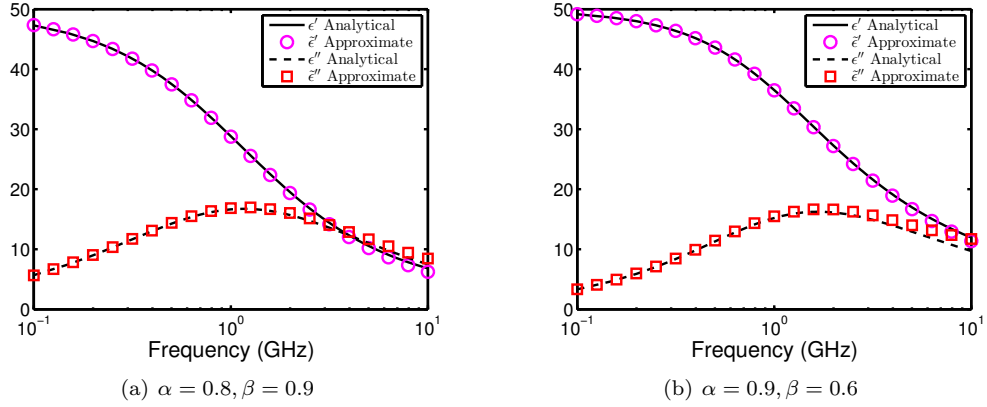


FIGURE 4.8. Real and imaginary part of the analytical complex relative permittivity and the approximate one of the H-N media.

REFERENCES

- [1] A. Alegria, L. Goitiandia, I. Telleria and J. Colmenero. α -relaxation in the glass-transition range of amorphous polymers. 2. Influence of physical aging on the dielectric relaxation. *Macromolecules*, 30(13): 3881–3888, 1997.
- [2] C. S. Antonopoulos, N. V. Kantartzis and I. T. Rekanos. FDTD method for wave propagation in Havriliak-Negami media based on fractional derivative approximation. *IEEE T. Magn.*, 53(6): 1–4, 2017.
- [3] P. Bia, D. Caratelli, L. Mescia, R. Cicchetti, G. Maione and F. Prudeniano. FDTD method for wave propagation in Havriliak-Negami media based on fractional derivative approximation. *Sign. Process.*, 107: 312–318, 2015.
- [4] K. Biswas, G. Bohannan, R. Caponetto, A. M. Lopes and J. A. T. Machado. Fractional-order models of vegetable tissues. In: *Fractional-Order Devices*, Springer, pp. 73–92, 2017.
- [5] M. F. Causley, P. G. Petropoulos and S. Jiang. Incorporating the Havriliak-Negami dielectric model in the FD-TD method. *J. Comput. Phys.*, 230(10): 3884–3899, 2011.
- [6] J. Chakarothei. Novel FDTD scheme for analysis of frequency-dependent medium using fast inverse Laplace transform and Prony's method. *IEEE Trans. Antennas Propagat.*, 67(9): 6076–6089, 2019.
- [7] K. S. Cole and R. H. Cole. Dispersion and absorption in dielectrics I. Alternating current characteristics. *J. Chem. Phys.*, 9(4): 341–351, 1941.
- [8] D. W. Davidson and R. H. Cole. Dielectric relaxation in glycerol, propylene glycol, and n-propanol. *J. Chem. Phys.*, 19(12): 1484–1490, 1951.
- [9] P. J. W. Debye. *Polar molecules*. Dover, 1929.
- [10] L. Demkowicz. *Computing with hp-ADAPTIVE FINITE ELEMENTS: Volume 1. One- and Two-Dimensional Elliptic and Maxwell Problems*. Chapman and Hall/CRC, 2006.
- [11] A. Z. Elsherbeni and V. Demir. *The Finite-Difference Time-Domain Method for Electromagnetics with MATLAB Simulations*. Edison, NJ, USA: SciTech, 2015.
- [12] A. Garcia-Bernabé, R. D. Calleja, M. Sanchis, A. Del Campo, A. Bello, and E. Pérez. Amorphous-smectic glassy main chain LCPs. II. dielectric study of the glass transition. *Polymer*, 45(5): 1533–1543, 2004.
- [13] R. Garrappa. Numerical evaluation of two and three parameter Mittag-Leffler functions. *SIAM J. Numer. Anal.*, 53(3): 1350–1369, 2015.
- [14] R. Garrappa, F. Mainardi and M. Guido. Models of dielectric relaxation based on completely monotone functions. *Fract. Calc. Appl. Anal.*, 19(5): 1105–1160, 2016.
- [15] R. Garrappa and G. Maione. Fractional Prabhakar derivative and applications in anomalous dielectrics: a numerical approach. *Lecture Notes in Electrical Engineering*, 407: 429–439, 2017.
- [16] A. Giusti, I. Colombaro, R. Garra, R. Garrappa, F. Polito, M. Popolizio and F. Mainardi. A practical guide to Prabhakar fractional calculus. *Fract. Calc. Appl. Anal.*, 23(1): 9–54, 2020.
- [17] R. Gorenflo, A. A. Kilbas, F. Mainardi and S. V. Rogosin. *Mittag-Leffler Functions, Related Topics and Applications*. Springer, Berlin, 2014.
- [18] S. Havriliak and S. Negami. A complex plane analysis of α -dispersions in some polymer systems. *J. Polym. Sci. C*, 14(1): 99–117, 1966.
- [19] S. Havriliak and S. Negami. A complex plane representation of dielectric and mechanical relaxation processes in some polymers. *Polymer*, 8: 161–210, 1967.
- [20] C. Huang and L.-L. Wang. An accurate spectral method for the transverse magnetic mode of Maxwell equations in Cole-Cole dispersive media. *Adv. Comput. Math.*, 45(2): 707–734, 2019.
- [21] D. F. Kelley. *Piecewise linear recursive convolution for the FDTD analysis of propagation through linear isotropic dispersive dielectrics*. Ph.D. thesis, Pennsylvania State University, 1999.
- [22] D. F. Kelley, T. J. Destan and R. J. Luebbers. Debye function expansions of complex permittivity using a hybrid particle swarm-least squares optimization approach. *IEEE T. Antenn. Propag.*, 55(7): 1999–2005, 2007.
- [23] A. A. Kilbas, M. Saigo and R. K. Saxena. Generalized Mittag-Leffler function and generalized fractional calculus operators. *Integr. Transf. Spec. F.*, 15(1): 31–49, 2004.
- [24] J. Li, Y. Huang and Y. Lin. Developing finite element methods for Maxwell's equations in a Cole-Cole dispersive medium. *SIAM J. Sci. Comput.*, 33(6): 3153–3174, 2011.
- [25] A. M. Lopes, J. T. Machado and E. Ramalho. Fractional-order model of wine. In: *Chaotic, Fractional, and Complex Dynamics: New Insights and Perspectives*, Springer, pp. 191–203, 2018.
- [26] C. Lubich and A. Schädle. Fast convolution for nonreflecting boundary conditions. *SIAM J. Sci. Comput.*, 24(1): 161–182, 2002.
- [27] W. McLean, V. Thomée and L. B. Wahlbin. Discretization with variable time steps of an evolution equation with a positive-type memory term. *J. Comput. Appl. Math.*, 69(1): 49–69, 1996.
- [28] L. Mescia, P. Bia and D. Caratelli. Fractional derivative based FDTD modeling of transient wave propagation in Havriliak-Negami media. *IEEE Trans. Microwave Theory Tech.*, 62(9): 1920–1929, 2014.
- [29] P. Monk. *Finite Element Methods for Maxwell's Equations*. Oxford University Press, 2003.
- [30] I. Podlubny. *Fractional Differential Equations: An Introduction to Fractional Derivatives, Fractional Differential Equations, to Methods of their Solution and some of their Applications*. San Diego, CA: Academic, 1999.
- [31] C. Polk and E. Postow. *Handbook of Biological Effects of Electromagnetic Fields*. CRC press, 1995.

- [32] T. R. Prabhakar. A singular integral equation with a generalized Mittag-Leffler function in the kernel. *J. Yokohama Math.*, 19: 7–15, 1971.
- [33] A. Quarteroni and A. Valli. *Numerical Approximation of Partial Differential Equations*. Springer, Berlin, 1994.
- [34] G. G. Raju. *Dielectrics in Electric Fields*. CRC Press, New York, 2016.
- [35] I. T. Rekanos. An auxiliary differential equation method for FDTD modeling of wave propagation in Cole-Cole dispersive media. *IEEE Trans. Antennas Propagat.*, 58(11): 3666–3674, 2012.
- [36] I. T. Rekanos. FDTD modeling of Havriliak-Negami media. *IEEE Microw. Wirel. Co.*, 22(2): 49–51, 2012.
- [37] I. T. Rekanos. FDTD schemes for wave propagation in Davidson-Cole dispersive media using auxiliary differential equations. *IEEE Trans. Antennas Propagat.*, 60(3): 1467–1478, 2012.
- [38] T. Repo and S. Pulli. Application of impedance spectroscopy for selecting frost hardy varieties of English ryegrass. *Ann. Botany*, 78(5): 605–609, 1996.
- [39] A. Schonhals. Fast calculation of the time dependent dielectric permittivity for the Havriliak-Negami function. *Acta Polym.*, 42(4): 149–151, 1991.
- [40] J. W. Schuster and R. J. Luebbers. An FDTD algorithm for transient propagation in biological tissue with a Cole-Cole dispersion relation. in *Proceedings of the IEEE Antennas and Propagation Society Int. Symp.*, 4: 1988–1991, 1998.
- [41] J. SHEN, T. TANG, AND L.-L. WANG, *Spectral methods: algorithms, analysis and applications*, vol. 41, Springer Science & Business Media, 2011.
- [42] A. Taflov and S. C. Hagness. *Computational Electrodynamics: The Finite-Difference Time-Domain Method*. Artech house, London, 2005.
- [43] F. Torres, P. Vaudon and B. Jecko. Application of new fractional derivatives to the FDTD modeling of pulse propagation in a Cole-Cole medium. *Microwave Opt. Technol.*, 13(5): 300–304, 1996.
- [44] K. Xu and S. Jiang. A bootstrap method for sum-of-poles approximations. *J. Sci. Comput.*, 55(1): 16–39, 2013.
- [45] F. Zeng, I. Turner and K. Burrage. A stable fast time-stepping method for fractional integral and derivative operators. *J. Sci. Comput.*, 77(1): 283–307, 2018.